Geochemical characteristics of hot springs in Southern Thailand

Poonnapa Klamthim

A Thesis Submitted in Partial Fulfillment of the Requirements

for the Degree of Master of Science in Geophysics

Prince of Songkla University

2022

Geochemical characteristics of hot springs in Southern Thailand

Poonnapa Klamthim

A Thesis Submitted in Partial Fulfillment of the Requirements

for the Degree of Master of Science in Geophysics
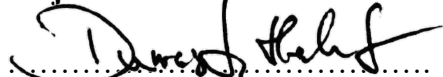
Prince of Songkla University

2022

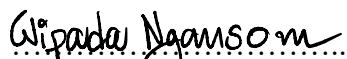**Copyright of Prince of Songkla University**

Thesis Title   Geochemical characteristics of hot springs in Southern Thailand

Author   Miss Poonnapa Klamthim

Major Program   Geophysics
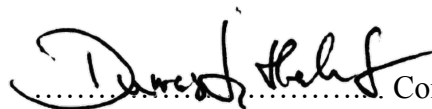

Major Advisor

....
(Asst. Prof. Dr. Helmut Dürrast)

Examining Committee

.... Chairperson
(Dr. Wipada Ngansom)

.... Committee
(Dr. Fabian Nitschke)
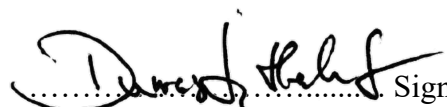
.... Committee
(Asst. Prof. Dr. Nararak Leesakul)

.... Committee
(Asst. Prof. Dr. Helmut Dürrast)

The Graduate School, Prince of Songkla University, has approved this thesis as partial fulfillment of the requirements for the Master of Science Degree in Geophysics

………………………….............................

(Asst. Prof. Dr. Thakerng Wongsirichot)

Acting Dean of Graduate School

This is to certify that the work here submitted is the result of the candidate's own investigations. Due acknowledgement has been made of any assistance received.

.... Signature

(Asst. Prof. Dr. Helmut Dürrast)

Major Advisor

.... Signature

(Miss Poonnapa Klamthim)

Candidate

I hereby certify that this work has not been accepted in substance for any degree, and is not being currently submitted in candidature for any degree.

..Poonnapa Klamthim.. Signature

(Miss Poonnapa Klamthim)

Candidate

ชื่อวิทยานิพนธ์   ลักษณะทางธรณีเคมีของน้ำพุร้อนในภาคใต้ของประเทศไทย

ผู้เขียน   นางสาวปุณณภา กล่ำทิม

สาขาวิชา   ธรณีฟิสิกส์

ปีการศึกษา   2565

บทคัดย่อ

น้ำพุร้อนสามารถพบได้ในทุกที่ทั่วประเทศไทยมีทั้งหมดประมาณ 120 แห่งโดยในภาคใต้ประกอบด้วยน้ำพุร้อนเกือบ 40 แห่ง ระบบของพลังงานความร้อนใต้พิภพในประเทศไทยเป็นระบบที่ไม่เกี่ยวข้องกับโครงสร้างทางธรณีวิทยาแบบภูเขาไฟดังระบบส่วนใหญ่ทั่วไปในโลกแต่เป็นระบบที่เกี่ยวข้องกับโครงสร้างหินร้อนที่อยู่ใต้ดิน น้ำพุร้อนส่วนใหญ่ถูกพัฒนาให้กลายเป็นสถานที่ท่องเที่ยวโดยเฉพาะสถานที่ท่องเที่ยวที่เกี่ยวกับสุขภาพ อย่างไรก็ตามการศึกษาทำความเข้าใจเกี่ยวกับพลังงานความร้อนใต้พิภพและการทำความเข้าใจถึงความสัมพันธ์ระหว่างสิ่งแวดล้อมทางธรณีวิทยากับลักษณะเฉพาะของน้ำพุร้อนมีความสำคัญอย่างยิ่งกับการพัฒนาแหล่งน้ำพุร้อนธรรมชาติ ในการศึกษาครั้งนี้ การสำรวจภาคสนามและการทดลองในห้องปฏิบัติการถูกนำมาศึกษาในการระบุลักษณะทางธรณีเคมีของน้ำพุร้อนใน 6 จังหวัดภาคใต้ประกอบไปด้วย จังหวัดกระบี่, จังหวัดนครศรีธรรมราช, จังหวัดพังงา, จังหวัดสุราษฎร์ธานี, จังหวัดชุมพรและจังหวัดระนอง การวิเคราะห์ธรณีเคมีของตัวอย่างน้ำพุร้อนในห้องปฏิบัติการได้ทำการวิเคราะห์ตัวอย่างน้ำที่ถูกเก็บมาจากน้ำ 3 แหล่งน้ำ ได้แก่ น้ำพุร้อน, น้ำบาดาล และน้ำทะเลทั้งในฝั่งอ่าวไทยและฝั่งอันดามัน ผลการวิเคราะห์พบว่าน้ำพุร้อนในภาคใต้มีอุณหภูมิของน้ำที่ผิวดินตั้งแต่ 35.7-70.0 องศาเซลเซียสและมีค่า pH อยู่ระหว่าง 6.6-8.1 จากปริมาณความเข้มข้นของไอออนประจุบวกและประจุลบในน้ำพุร้อนทำให้สามารถจำแนกกลุ่มของน้ำพุร้อนตามลักษณะเด่นของไอออนออกมาได้เป็น 4 กลุ่ม ได้แก่ $1.Na^+-Cl^-$, $2.Na^+-Mg^{2+}-HCO_3^-$, $3.Ca^{2+}-HCO_3^-$, และ$4.Ca^{2+}-SO_4^{2-}$ อีกทั้งคาร์บอเนตที่เป็นองค์ประกอบในน้ำพุร้อนมีที่มาจากสองแหล่งคือ การผุกร่อนและการละลายของหินปูนและหินโดโลไมต์ที่อยู่รอบๆบริเวณของน้ำพุร้อน ยิ่งไปกว่านั้น ความเข้มข้นของ Na^+, Cl^- และ Mg^{2+} ยังเป็นสิ่งที่บ่งบอกถึงการเจือปนของน้ำทะเลในฝั่งอ่าวไทยและฝั่งอันดามันภายในแหล่งน้ำร้อนอีกด้วย จากผลการวิเคราะห์ผลไอโซโทปเสถียรและปริมาณความเข้มข้นของสารคาร์โรฟลูออโรคาร์บอนพบว่าน้ำร้อนใต้พิภพในภาคใต้ของประเทศไทยส่วนใหญ่มาจากน้ำใต้ดินที่มีอายุมากผสมกับน้ำจากบรรยากาศที่ถูกเติมลงไปในระบบน้ำบาดาลด้วยการเดินทางผ่านชั้นหินจากพื้นผิวลงไปสู่แหล่งเก็บน้ำจากนั้นน้ำจะได้รับความร้อนจากพลังงานความร้อนใต้พิภพและพุขึ้นมากลายเป็นน้ำพุร้อน

Thesis Title   Geochemical characteristics of hot springs in Southern Thailand

Author   Miss Poonnapa Klamthim

Major Program   Geophysics

Academic year   2022

Abstract

Hot water springs can be found in most regions of Thailand, from the north to the south, except in the northeast. There are around 120 hot springs altogether, with about 40 hot springs in Southern Thailand, and all are related to a non-volcanic geological setting. Most hot springs are mainly developed as tourist destinations, for local as well as for international visitors, often combined with spas or other health-related activities. However, for any further development, including geothermal energy, but not limited to, a better understanding of relationships between the geological environment and hot water characteristics is required. In this study, field investigations and laboratory measurements were carried out to identify the hydrogeochemical signatures of major hot springs in Southern Thailand, with locations in Krabi, Nakhon Si Thammarat, Phang Nga, Surat Thani, Chumphon, and Ranong Province. Standard and advanced geochemical analysis of water samples was done in laboratories in Thailand and in Germany; water samples were collected from natural hot springs, groundwater wells, and seawater sources along the eastern (Gulf of Thailand) and western coast (Andaman Sea) of Southern Thailand. Results show that hot springs discharge geothermal water with temperatures between 35.7 to 70.0 °C and mostly have an alkaline pH of around 6.6 to 8.1. Hot springs in Southern Thailand separated into two main systems which are hot spring in igneous area and in sedimentary area. The major cation and anion concentrations indicate that hot springs in the Southern Thailand can be separated and classified into four types: Na^+-Cl^-, Na^+-Mg^{2+}-HCO_3^-, Ca^{2+}-HCO_3^-, and Ca^{2+}-SO_4^{2-} rich type. Carbonate components in the water originated from weathering and dissolution of carbonate and dolomite formations nearby hot springs. Moreover, elevated salinity concentrations (Na^+, Cl^-, Mg^{2+}) in some of the hot springs can be correlated to seawater intrusion from the Andaman Sea in the west or the Gulf of Thailand in the east. Oxygen stable isotope data and CFC concentration display reveals that the pathway of geothermal water in Southern Thailand is mainly from old local precipitation water that accumulated in the system before the 1950s and then mixed with low proportion of recharged fresh meteoric water from the 2010s going downwards into the subsurface and heated up by heat sources and finally to be discharged at the subsurface as a hot spring.

ACKNOWLEDGEMENT

CONTENTS

CONTENTS (CONTINUED)

LIST OF TABLES

LIST OF FIGURES

LIST OF FIGURES (CONTINUED)

LIST OF FIGURES (CONTINUED)

CHAPTER 1

INTRODUCTION

1.1 Introduction

Hot springs or geothermal springs are springs in which normal groundwater is geothermally heated by an underground heat source and emerges as hot water to the surface with a temperature significantly higher than the mean annual temperature of the air of the surrounding area (Affaro, 1994). Most water of such a hot spring system comes from rain that seeps deep into the ground until it reaches an aquifer, thus called groundwater. This groundwater is heated by hot rocks, rises through fractures, cracks, and faults in the earth's crust, and emerges to the surface as hot springs. The possible natural heat source of geothermal water depends on its geological structure. In volcanic areas, very hot rocks heated by magma come into contact with groundwater. However, in non-volcanic areas, the water contacts underneath hot rocks with the geothermal gradient or granite intrusion (Anuar et al., 2021). Geothermal water is mostly managed as a recreation spot related to healthy activities for tourism. Furthermore, the high potential hot springs with surface temperatures up to 95°C developed for electricity power production since the geothermal resource is an efficient renewable energy with a low carbon footprint (Anuar et al, 2021; Ghoddousi et al., 2021; Oyuntsetseg et al., 2015).

Hot springs can be found in most regions of Thailand, from the north to the south, except in the northeast, with around 120 hot springs altogether. Northern Thailand has 50 known hot springs mainly in Mae Hongson, Chiang Rai, Chiang Mai, Lamphun, Lampang, Tak, and Phrae. In the central and eastern part of Thailand, there are about twenty hot water springs, in Sukhothai, Phetchabun, Kamphaengphet, Uthaithani, Kanchanaburi, Lopburi, Ratburi, Petchburi, and Chonburi provinces. Southern Thailand has about 40 hot springs in Chumphon, Ranong, Surat Thani, Phang Nga, Krabi, Phuttalung, Satul, Yala, Trang, and Nakhon Si Thammarat provinces. Most hot springs are dominantly developed as tourist destinations. In Thailand, there are five high-potential geothermal energy sources in Chiang Mai, Chiang Rai, and Phrae. The only hot spring in northern Thailand with a capacity of 100 Watts is used for power

generation is the Fang Hot spring at Chiang Mai (Charusiri et al., 2003). However, for further development, especially in geothermal energy, natural resource management and a better understanding of natural and the relationship between the geological environment and hot water characteristics are required to allow better utilization of finite resources.

1.2 Literature review

1.2.1 Geology of Southern Thailand

Southern Thailand lies on a narrow peninsula between the Gulf of Thailand on the east coast and the Andaman Sea on the west coast with a political boundary to Malaysia to the south. According to Figure 1.1, there are two major fault zones that traverse the peninsula from west to east; first the Ranong Fault Zone, and the second is the Klong Marui Fault Zone, which crosses the peninsula further south, separating the Upper and Lower Peninsulas. The upper part covers Ranong, Chumphon, Phang Nga, Phuket, and the northern part of Surat Thani provinces. It mainly consists of Permian shale that lies along Chumphon to Phuket and has intrusion of granitic rocks in some areas.

The western coast of the peninsula is a submerged coastline with predominantly has marine and colluvial deposits due to the high mountainous terrain between Thailand and Myanmar in the northwest. Limestone and dolomitic limestone additionally seem in Chumphon, and they may be discovered near granite bodies in the northwest of Surat Thani. However, the lower part covers Surat Thani to Yala, the southernmost province in Thailand. There are typically Cenozoic sedimentary deposits and sandstones. There are granite mountains range extending from Nakhon Si Thammarat to Satun and also some limestone outcrops close to the mountain range. The East Coast is generally a coastline made up of marine sediments and clays (Nazaruddin et al., 2021; Ngansom et al., 2019).
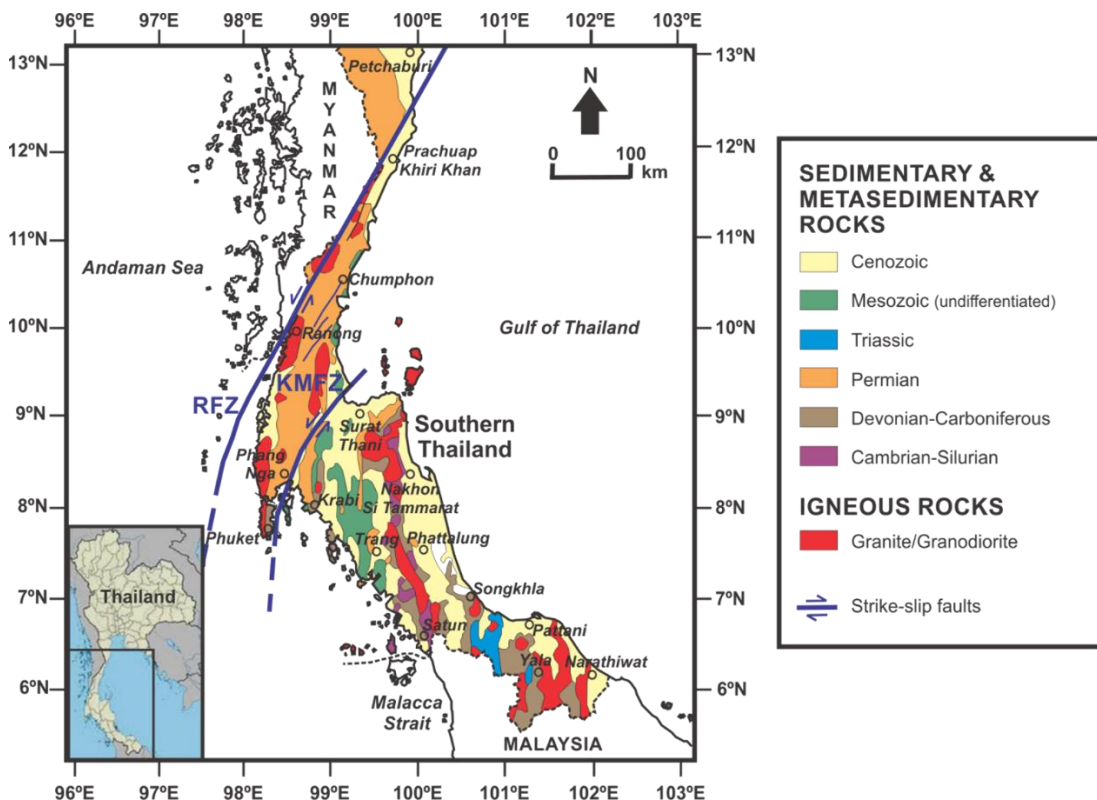
Figure 1.1 Geology map of Southern Thailand with two major fault zones including RFZ: Ranong fault zone and KMFZ: Khlong Marui fault zone.

1.2.2 Groundwater

Groundwater is fresh water from rain that is stored beneath the Earth's surface in the pore spaces of sedimentary rocks, both unconsolidated and consolidated, in weathered layers, in hard rock fractures of and fault zones, as well as in karst caves (see (Alaska Department of Environmental Conservation, 2009; Figure 1.2). Groundwater comes from rain drops, which penetrate down into the subsurface passing between the particles of soil, sand, gravel, or rock until they reach a depth level where the subsurface is filled with water, the so called water table. Groundwater stored in permeable rocks called aquifers. An aquifer is a subsurface formation of permeable rock, which can be a layer of sand, sandstone, limestone or fractured rock. Groundwater is found in two zones: the unsaturated zone, an upper zone, which contains mostly air in open pore space and the saturated zone, a deeper zone, which is filled with water in all pore space. These two zones are separated by the top of accumulated water level in saturated zone called the water table. Groundwater, utilized by constructing wells, is often used for

agricultural and industrial purposes, and it is a source of drinking water and also the largest freshwater in the hydrological cycle (Alaska Department of Environmental Conservation, 2009).
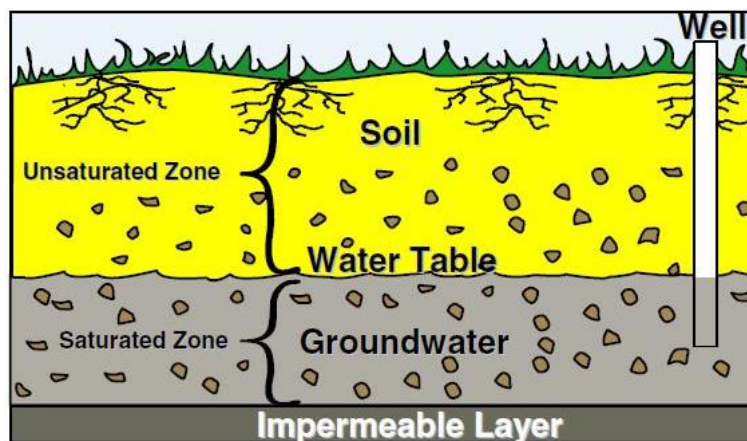
Figure 1.2 Groundwater zone (from Alaska Department of Environmental Conservation, 2009).
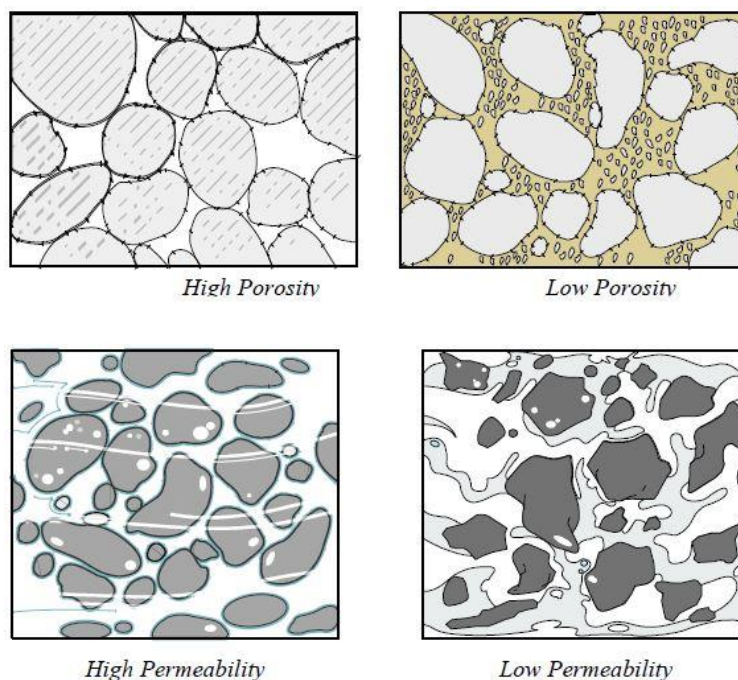
Figure 1.3 Different arrangements of grains resulting in different porosity and permeability (Alaska Department of Environmental Conservation, 2009).

Water from rain and snowmelt seeps through the unsaturated zone into aquifers, which are geological formations of sediments and rocks. It is an area that is permeable to groundwater flow enough for wells and springs (Figure 1.3). Aquifers also can receive water from surface waters such as lakes. The speed of groundwater move through the material is determined by the permeability of rock. Moreover, the amount of water in aquifer depends on the porosity in material that can fill with water (Christopherson, 2012).

1.2.2 Geothermal system

A geothermal system mainly consists of three main parts (Figure 1.4). The first part of the system is the thermal energy. The source of thermal energy in groundwater is different between the two levels of water. The energy within the shallow groundwater is basically from the sun and the power in the deeper water is derived from upward heat from the Earth's interior.
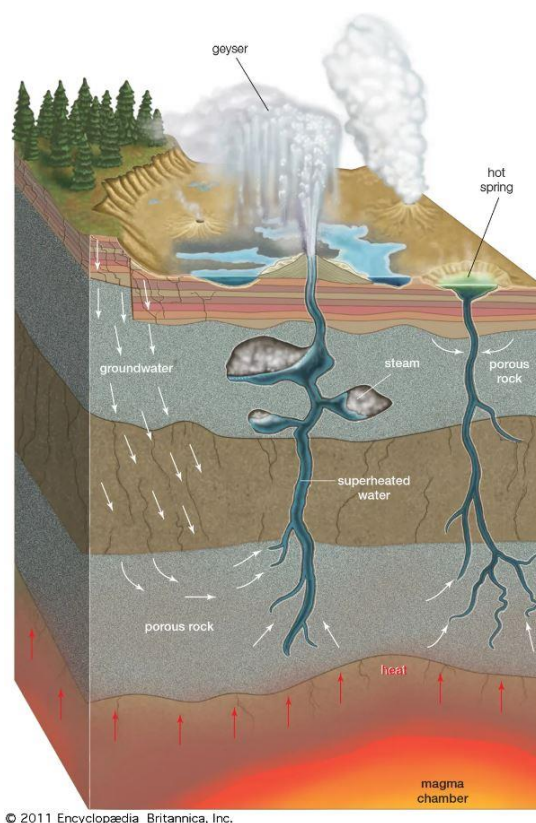
Figure 1.4 Occurrence of a geothermal system with a geyser and hot spring (from Britannica, 2021).

Natural heat sources possible from (1) an intrusive magma rising to heat the surrounding rock relatively closer to the surface, (2) the extrusion of igneous rock in a volcanic area, (3) a radioactive element such as uranium (U), thorium (Th), and potassium (K), (4) heat generated by the friction along faults, and (5) deep hot rocks heated with the geothermal gradient. The second is the permeable structure underneath the surface which provided the groundwater reservoir covered with impermeable cap rock. The last component is groundwater which is recharged from surface sources or shallow aquifers seeping into the ground and gaining heat from the sources. Groundwater is prevented from rising by an impervious layer under the pressure. In high permeability zones, heated water in liquid or vapor form depending on their temperature with high pressure and low density due to the heat being forced to flow through cracks, fractures, or faults and reaches the surface where it forms springs (Alfaro et al., 1994).

A geyser thermal spring is one kind of geothermal water that intermittently spouts hot water and steam into the air and often occurs in a volcanic area (Figure 1.4). The steam results from the expansive pressure of superheated steam within a confined subsurface pathway. When the water in an aquifer is heated above the boiling point, the pressure increases, and then the steam accelerates upward and flushes into the surface.

1.2.3 Hot springs in Thailand

Department of Mineral Resources of Thailand reports 112 hot springs in Thailand with discharge temperatures ranging from 40-100 °C and appear in all parts of the country except in the northeastern part (Figure 1.5). The hot springs were divided into three groups: high, medium, and low. In high-potential hot springs, the surface water temperature is 80 °C or higher. Medium potential hot springs refer to surface water temperatures between 60 and 80 °C, and low potential hot springs refer to surface water temperatures below 60°C. All hot springs are related to a non-volcanic origin but occur in sedimentary and granitic settings. Chemical analysis revealed the hot spring pH range from 6.4–9.5 and mostly contains less total dissolved solids (TDS). Hot springs from the north have commonly more potent mineral constituents. The range of the TDS and anion ion of thermal water in northern Thailand varies to a large degree than in the south.
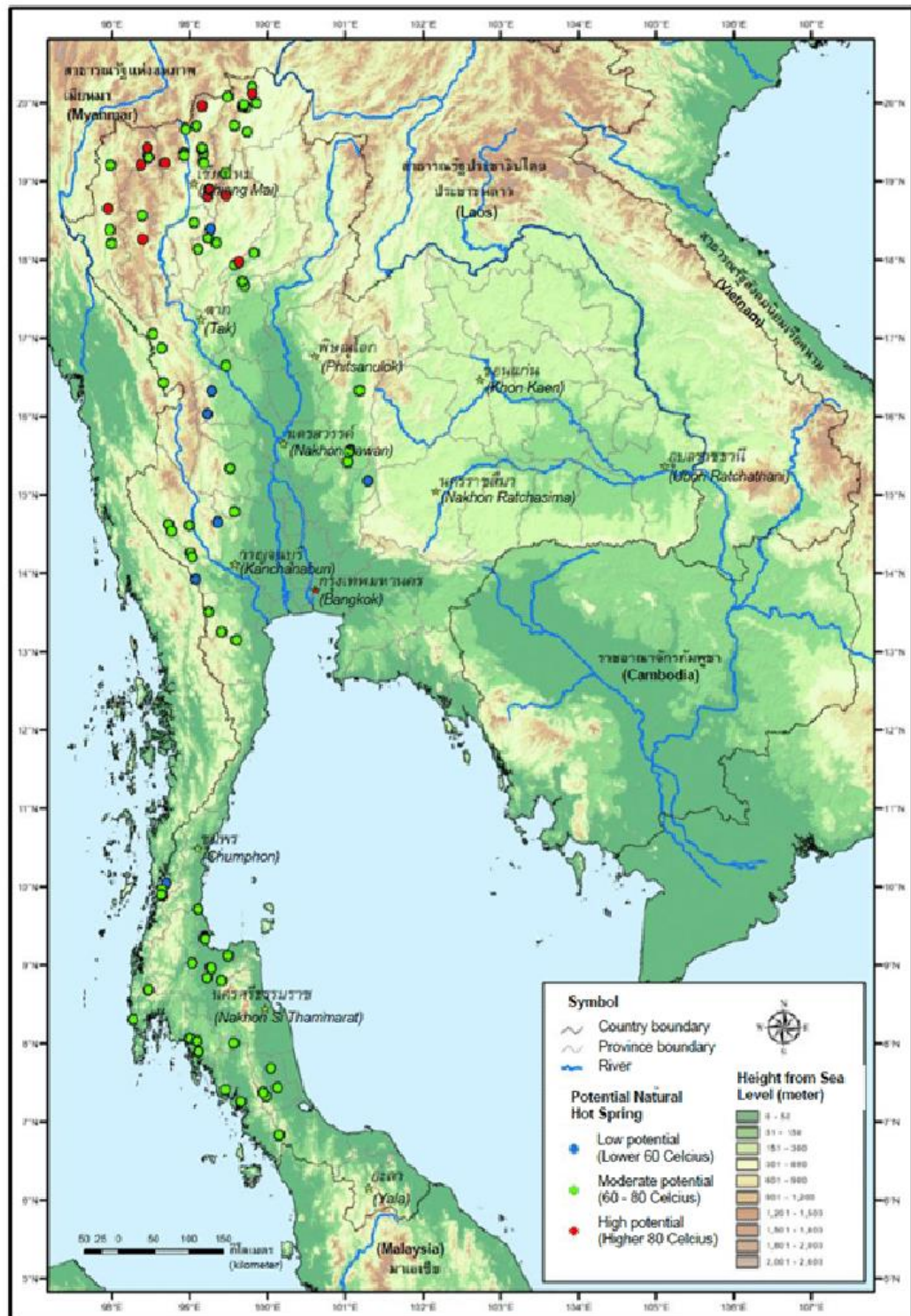
Figure 1.5 Location map of hot springs in Thailand with three classifications: Low potential in blue dot, Moderate potential in green dot, and High potential in red dot (Chaiyat et al., 2014).

Hot springs in northern Thailand are considered as a high potential and they are classified as moderate enthalpy with surface temperature from 60-99 °C and reservoir temperature ranges of 180-210 °C, while others are low enthalpy and discharge thermal water with a temperature that varies from 55-85 °C (Figure 1.5). The thermal water possibly heat sources separate into two types: First, water heated within the granitic rock, and second is heated with deep burial granitic rock that is covered by permeable rock. Therefore, Fang hot spring in Chiang Mai is the only hot spring in Thailand developed into a small-scale power plant by the Electricity Generation Authority of Thailand (EGAT). Other hot springs are dominantly developed recreational for tourism and minority for heating, agriculture, and industrial (Chaiyat et al., 2014; Charusiri et al., 2000; Raksaskulwong et al., 2008).

1.2.3 Geothermal water investigation
Geochemical investigation

Groundwater in the thermal system accumulates in the reservoir and after heating, it travels upward to discharge through the surface carrying the ion components and minerals making differences in chemical characteristics in each thermal system and environment. The chemical characteristics of the groundwater provide information about its geological history, geological setting, and its influence on the water-rock interaction through the pathway that it has passed (Kwansirikul et al., 2005). The chemical properties of the groundwater mainly consider the concentration of common ions in groundwater which are cations and anions including Ca^{2+}, Mg^{2+}, Na^+, K^+, Cl^-, SO_4^-, CO_3^{2-}, HCO_3^-, NO_3^-, and F^-, and the total dissolved solids or TDS.

Chemical classifications

Diagrams and contour plots are often used to model water chemistry data to determine groundwater quality and classify groups of hot springs. A Piper diagram is a graphic procedure to divide relevant analytical data to classify the concentration of the dissolved constituents in water by drawing two triangles corresponding with the cations and anions, respectively. Then another diamond is used that summarizes both triangles, as shown in Figure 1.6. The base of the left triangle is calcium (Ca^{2+}), the left is magnesium (Mg^{2+}), and the right is sodium and potassium ($Mg^{2+}+K^+$) axes. For anions,

the bottom is the chloride and fluoride (Cl⁻+F⁻), left is the carbonate and bicarbonate (CO_3^{2-}+HCO_3^-), and the right is the sulfate (SO_4^-) axis.
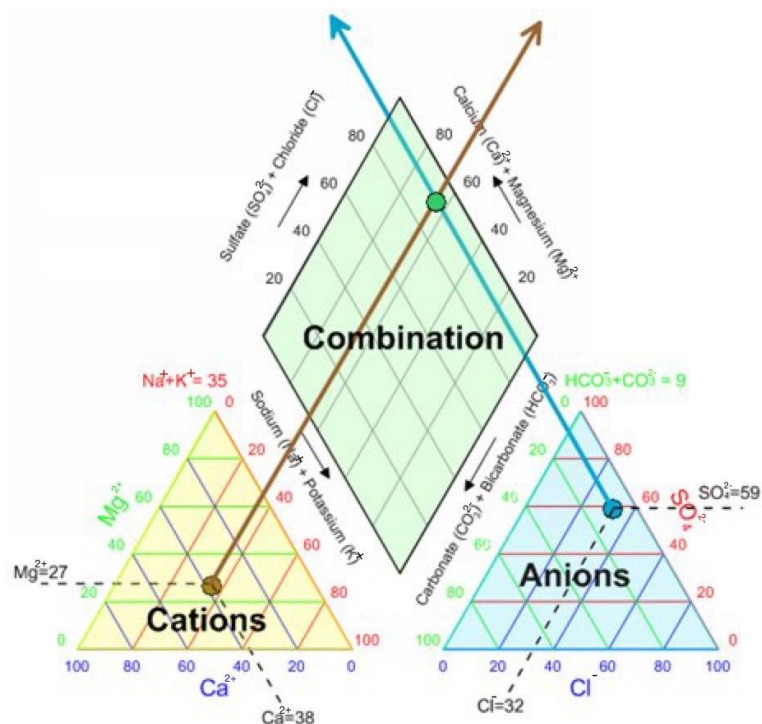
Figure 1.6 Three components of a Piper plot. Bottom left is a plot for cations, bottom right is for anions, and top is a diamond plot of projections from the other two plots.

In Figure 1.7, the hydrochemical facies can be identified based on the locations of the hot spring samples on Piper's diamond plot and it can divide water into four simple types. Samples at the top of the diamond are high in Ca^{2+}+Mg^{2+} and Cl^-+SO_4^{2-} and are calcium sulfate waters, samples in the left corner are rich in Ca^{2+}+Mg^{2+} and HCO_3^- called calcium bicarbonate waters, and samples lying near the right side are sodium chloride waters, and samples in the lower of diamond are primarily composed of alkali carbonates which are rich in Na^++K^+ and CO_3^{2-}+HCO_3^- (Jankowski et al., 1991; Singh et al., 2015; Ngansom et al., 2022).
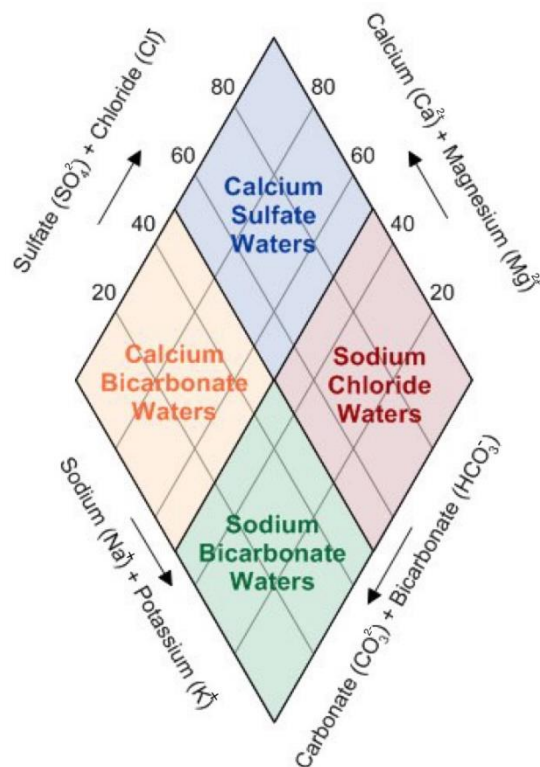
Figure 1.7 Chemical facies of water samples due to their location.

Saline water intrusion identification

　　　　Groundwater is the dominant recharged water in the geothermal system. Groundwater quality in coastal areas is often especially affected by seawater intrusion. As a result, salinization will increase the chemical composition of groundwater, especially the concentration of dissolved solids (TDS), and increase in Cl^-, Na^-, Mg^{2+}, and SO_4^{2-} (Kumar, 2016). Na^- and Cl^- have a certain role in the salinization process in the coastal regions. The concentrations of Cl^- were plotted against major ions with the mean seawater dilution line shown in Figure 1.8. If the ratio of Cl^- and ion are close to the seawater trend, the salinity of hot spring water is clearly of marine origin. Figure 1.8a-b show an example of water samples that lies in the same ratio as the seawater line. Furthermore, the discharged temperature of the water sample increase with the Cl^- contents in Figure 1.8h indicating that the saline solution is part of the hot component of the mixture (Duriez et al., 2008).
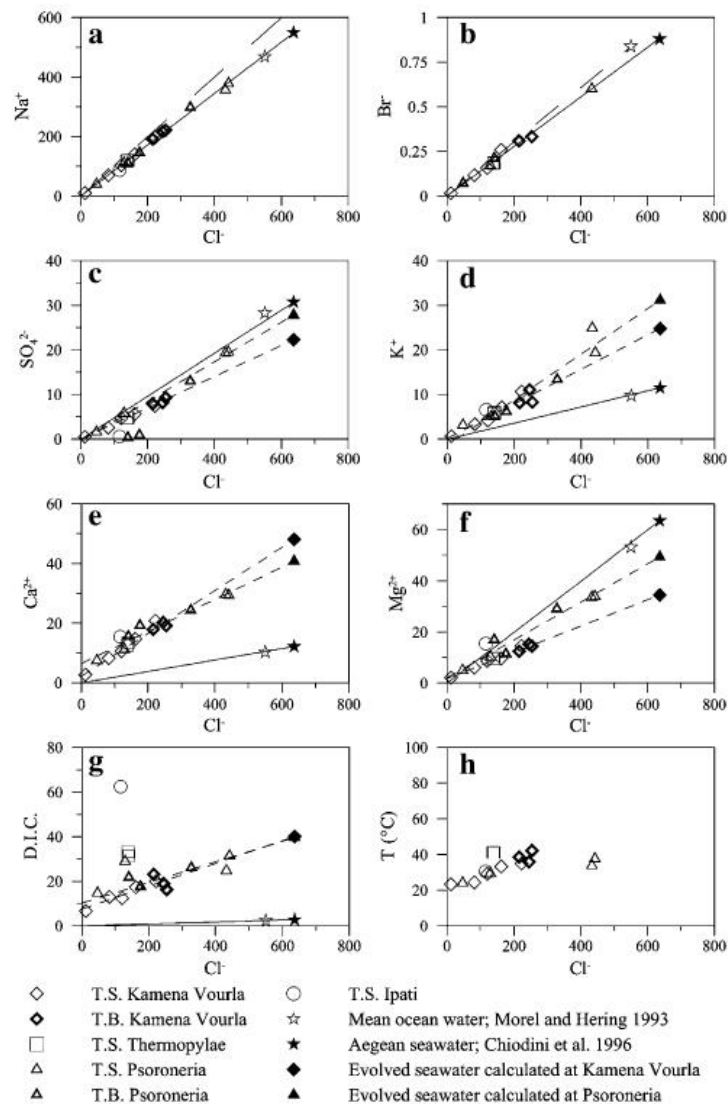
Figure 1.8 Major ions and temperature versus Chloride content of thermal water with the seawater dilution line or solid line (Duriez et al., 2008).

Origin of carbonate components

The groundwater chemical components of aquifers typically reflect the chemical composition of the dominant geological rock or sediment type in the surrounding recharge areas. Rock–water interaction, weathering, and dilution caused by water precipitation in reservoirs are the natural processes that control the carbonate contents in groundwater. Rock with high carbonate consists of limestone, dolomitic limestone, and dolomite. The major carbonate ions in groundwater are generally calcium, magnesium, and bicarbonate ions. If the ratio of Ca^{2+}/Mg^{2+} concentration is

equal to 1, dissolution of dolomite exists, while a higher ratio indicates a greater contribution of calcite minerals dissolution (Cerar et al., 2013).

The relationship of $Ca^{2+}+Mg^{2+}$ versus $HCO_3^-+SO_4^{2-}$ was used to identify carbonate origin based on the position of the water sample in the diagram plotted of $Ca^{2+}+Mg^{2+}$ and $HCO_3^-+SO_4^{2-}$ compared with the 1:1 line shown in Figure 1.9. The samples plot close to the 1:1 equiline shows that calcite and dolomite dissolution is the main carbonate origin. If the samples have an excess of Ca^{2+} or Mg^{2+}, their concentration can be a result of reverse ion exchange. Besides that, carbonate and silicate mineral weathering such as feldspar make the water samples position in an excess of $HCO_3^-+SO_4^{2-}$ (Cesar et al., 2013; Oyuntsetseg et al., 2015; Wen et al., 2012; Zaidi et al., 2015).
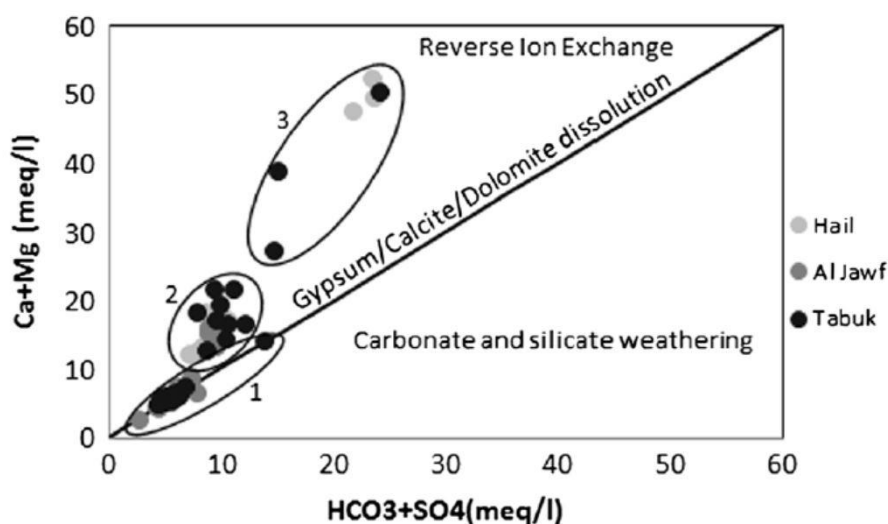
Figure 1.9 Relationship of ion concentration between $Ca^{2+}+Mg^{2+}$ versus $HCO_3^-+SO_4^{2-}$ (Zaidi et al., 2015).

Stable isotope in groundwater

The most commonly used isotopes in studies of geothermal systems worldwide are oxygen (O), hydrogen (H), carbon (C), and helium (He). Stable isotopes of hydrogen occurring naturally are ^1H (hydrogen) and D (deuterium), those of oxygen are ^{16}O, ^{17}O, and ^{18}O; carbon and helium each have two stable isotopes which are ^{12}C and ^{13}C, ^3He and ^4He, respectively (Nicholson, 1993). Stable isotope studies are based on the use of isotope ratios of the most abundant isotopes ($^{18}O/^{16}O$). In geochemical

applications, stable isotope compositions of H, O, and C are displayed in terms of deviations of their isotope ratios from the ratio of the reference standard. The variations in D/H and $^{18}O/^{16}O$ isotopic ratios in water samples are expressed as per mil (‰) deviation with respect to standard mean ocean water (VSMOW) which is

$$\delta\text{‰} = \frac{\text{Rsample} - \text{RSMOW}}{\text{RSMOW}} \times 1000 \text{.................................. (1.1)}$$

where R is the isotopic ratio of $^{18}O/^{16}O$ or D/H. The data of δ-values for water precipitation in Thailand are accessible online in the framework of the Global Network of Isotopes for Precipitation (GNIP) and are given in the mean monthly values. The meteoric water baseline for Thailand is slightly different from the global meteoric water line because of the difference in the evaporation of water and the amount of humidity. Thailand's meteoric water baseline described as

$$\delta D = 7.35\delta^{18}O + 6.11 \text{ , with } R^2 = 0.972\text{........................... (1.2)}$$

Figure 1.10 shows the comparison of Thailand meteoric water baseline and global meteoric water baseline with groundwater samples (white dot). The water samples was located close to the meteoric baseline indicating that groundwater samples recharge from local meteoric precipitation and infiltration (Kwansirikul et al., 2005; Hartantoo et al., 2022).
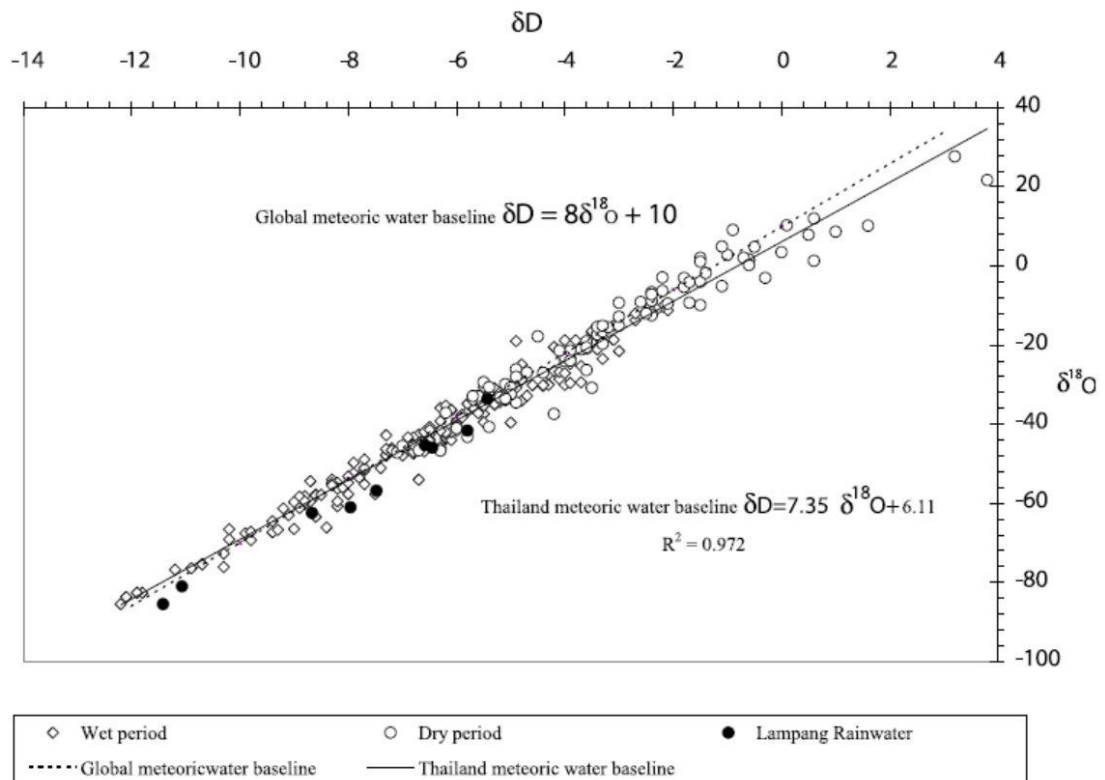
Figure 1.10 Thailand Meteoric Water Baseline and global meteoric water baseline with groundwater samples (Kwansirikul et al., 2005).

Groundwater dating

Groundwater age is not an absolute age of water, but it is a measure of the recharge year of a groundwater resource. A natural tracer for groundwater can be any component or property of groundwater that can be measured. Chlorofluorocarbon (CFC) and sulfurhexafluoride (SF_6) measurements are one of the tracers used to identify groundwater age and contaminant water sources since they are widespread across the Earth's surface, they can dissolve in water, and the release rate is known. CFC was produced for use in refrigeration in 1930s and further used in air-conditioning, insulation, and in the electronics industry. While SF_6 was used for electrical and thermal insulation since the 1950s. The concentration of CFC went up until the 1990s as shown in Figure 1.11 when the Montreal Protocol ordered limiting CFC production as CFC are a factor affecting the greenhouse effect by destroying the ozone layer. However, contamination of CFC and SF_6 in water is useful to trace the water source and the recharge water age (Chambers et al., 2019; Plummer et al., 2006).
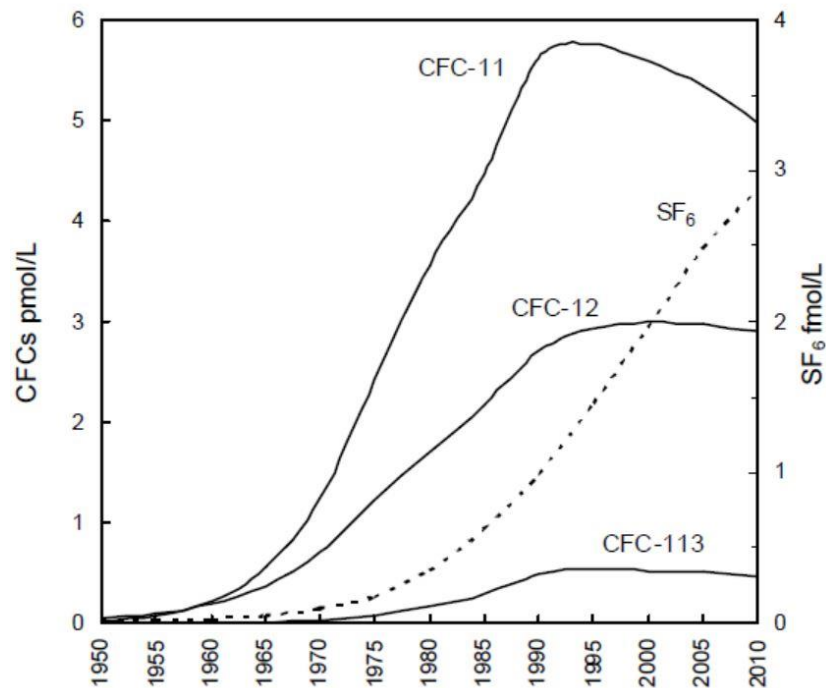
Figure 1.11 Variation in concentration of CFC and SF_6 over time in Groundwater (Darling et al., 2010).

The recharge age of groundwater is determined by comparing the concentration of CFC-11 (trichlorofluoromethane), CFC-12 (dichlorodifluoromethane), CFC-113 (trichlorotrifluoroethane), and SF_6 in groundwater with the particular CFC concentration known as the piston flow. These can be described in case of no mixing process in the groundwater sample. Therefore, solving the mixing in groundwater, CFC-11 is plotted against each other with CFC-12 and CFC-113 displayed in Figure 2.12. The piston flow (solid line) shows an unmixed sample recharged in a different year and the binary mixing (dash line) indicates the proportion of water recharged and CFC-Free water. Sample water that is located in Point B means there is a mixture in a 50:50 ratio between the recharged water in 1985 and old, CFC-free water (Plummer et al., 2006).
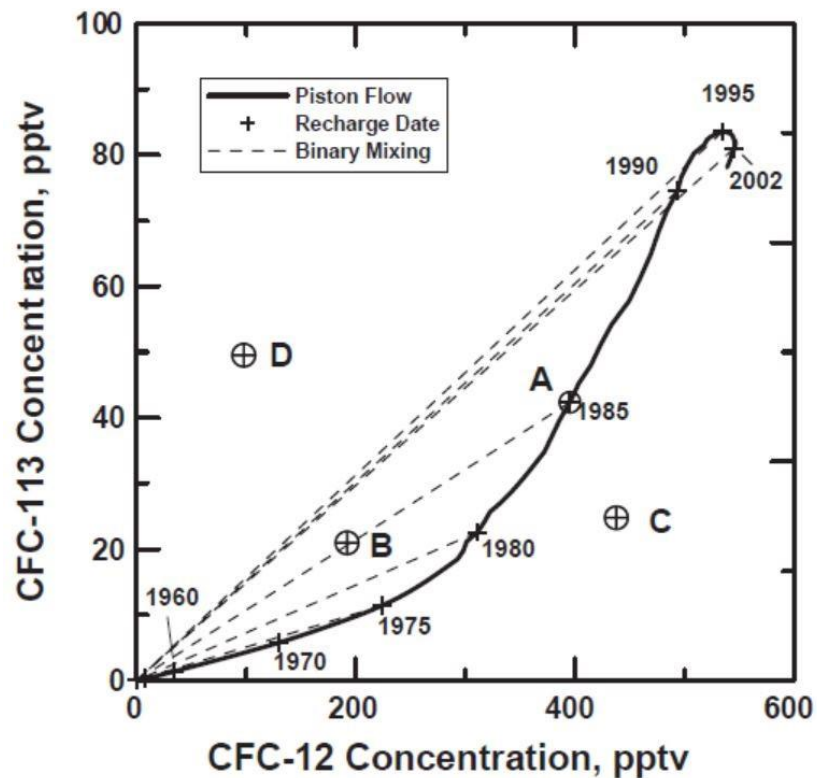
Figure 1.12 Plot of CFC-113 versus CFC-12 concentrations with water samples positioned in point A and point B (Plummer et al., 2006).

1.3 Objectives

In this study, field investigations and laboratory measurements were carried out to define the geochemical characteristics and signatures of major geothermal systems in Southern Thailand and to identify the influence of groundwater and seawater in the thermal system.

CHAPTER 2
RESEARCH METHODOLOGY

2.1 Geological survey

Geological surveys were conducted in nine provinces of Southern Thailand before collecting water samples, Satun, Phatthalung, Trang, Nakhon Si Thammarat, Krabi, Surat Thani, Phang Nga, Ranong and Chumphon, to understand the geology of the areas and to explore hot spring locations. This method provides information about sediment and rock types, and also give a detail about the possibility to access and sample hot springs. The goal of the geological surveys was to understand the geology, hydrology, and petrology of the study area in order to select sampling sites and to obtain more data related to the hot springs system.

2.2 Sampling locations

For this research, altogether 17 thermal springs in six provinces of Southern Thailand were chosen, including six hot spring samples from Krabi (KB), one sample from Nakhon Si Thammarat (NS), three samples from Phang Nga (PG), three samples from Surat Thani (SR), one sample from Chumphon (CP), and three samples from Ranong (RN). In addition, two groundwater samples were collected in village wells in Krabi and Ranong province, and two seawater sources were also collected along the eastern (Gulf of Thailand) and western coast (Andaman Sea). The location of the hot spring samples, groundwater samples and seawater samples are shown in Figure 2.1.
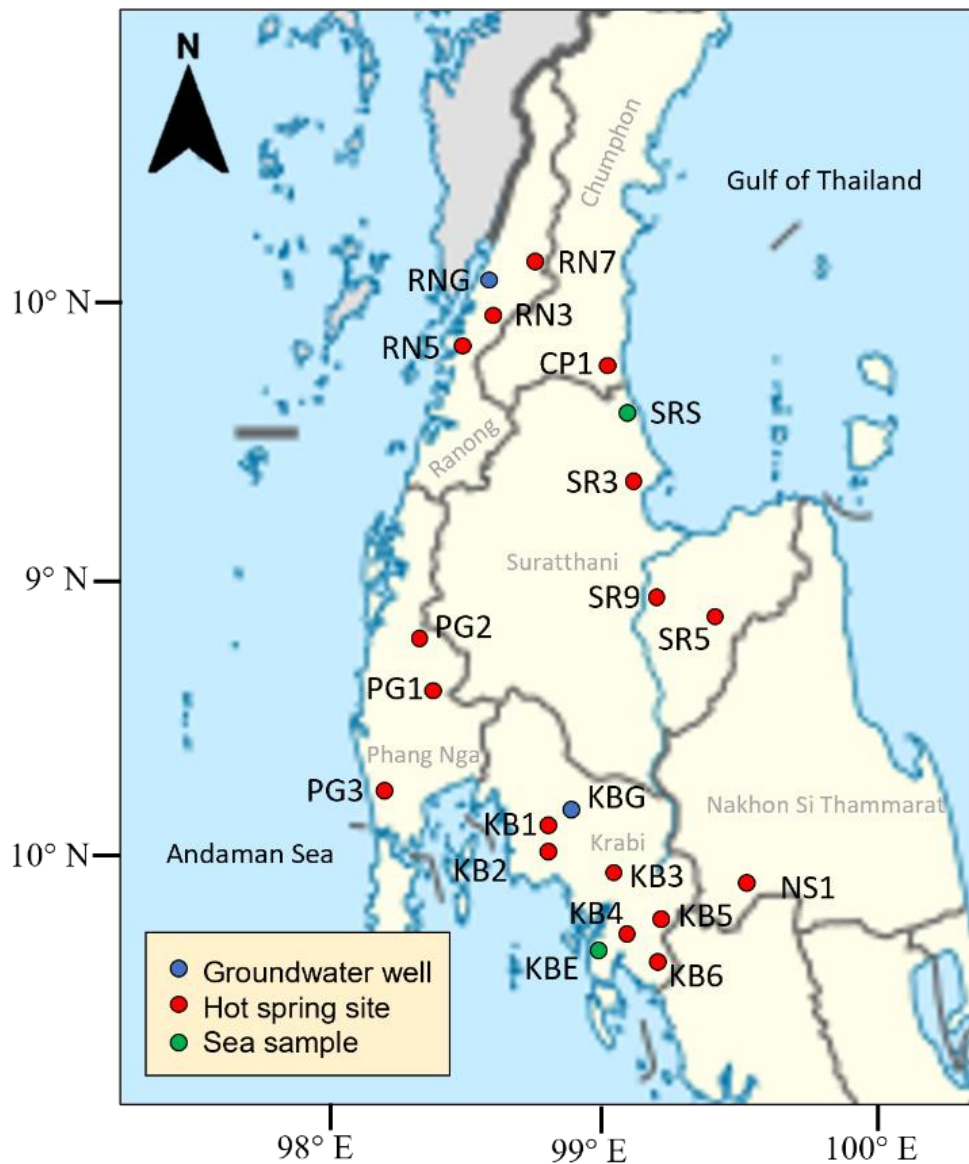
Figure 2.1 Location of sampling sites, hot spring sites, groundwater wells, and sea water samples: KB-Krabi, NS-Nakhon Si Thammarat, PG-Phang Nga, SR-Suratthani, CP-Chumphon and RN-Ranong.

2.3 Sampling equipment

The equipment that uses to measure on-site parameters consist of following items as shown also in Figure 2.2:

1) pH meter
2) Conductivity meter
3) Thermometer
4) Alkalinity test set
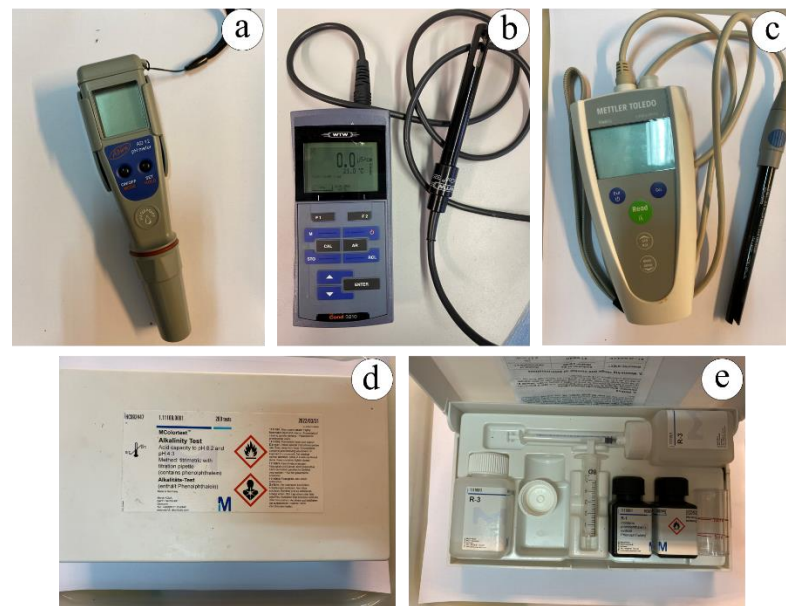
Figure 2.2 Equipment for on-site measurements: a) pH meter, b) conductivity meter, c) thermometer and d), e) alkalinity test set.

The equipment used to collect water samples for major anion, cation and isotope concentration analysis is

1) Low-density polyethylene bottle 25 ml
2) Syringe with filter holder
3) 0.45 μm filter paper
4) Concentrated hydrochloric acid (HCl)
5) Brown glass bottle 5 ml
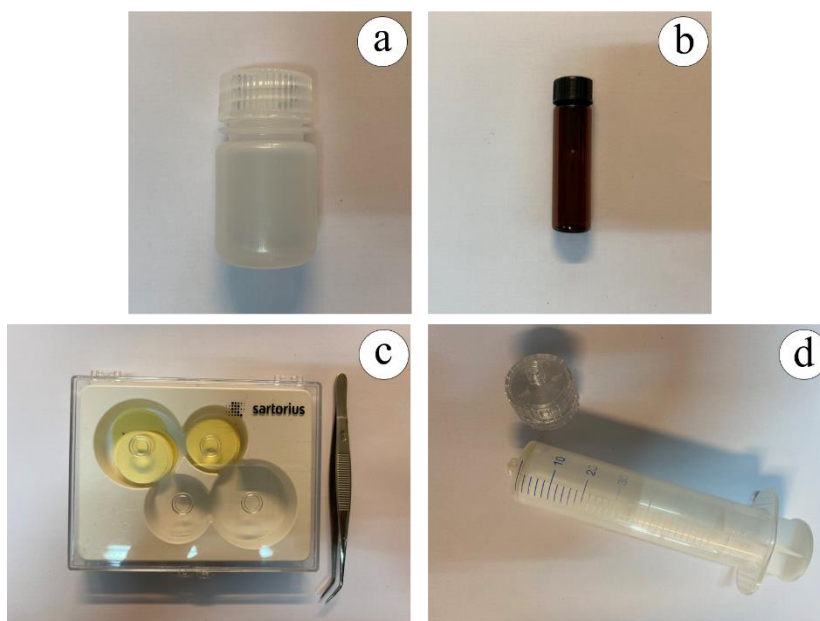
Figure 2.3 Pieces of equipment for collecting water samples: a) Low-density polyethylene bottle 25 ml, b) brown glass bottle 5 ml, c) 0.45 μm filter paper and d) Syringe with filter holder.

In the case of CFC-SF$_6$ concentration analysis, a special container has been used to collect the water sample. It consists of the following equipment (see also Figure 2.3):

1) Brass sampling container
2) Glass sampling bottle with plug and safety clip
3) Water pump
4) Tube
5) Bucket

Figure 2.4 Water sampling container for CFC-SF$_6$ concentration analysis consists of five items: brass container with lid, glass bottle with plug and safety clip, water pump, tube and bucket.

2.4 Sample collection

At each hot spring the sampling point is at the hottest spring or the hottest outflow location of the spring. If the sample is taken from a pool, the sampling location was in the area with the highest temperature. The process of water sampling is separated into two parts. The first part is on-site measuring. At the sampling site, pH, conductivity, and temperature of outflow water were measured using a pH meter, conductivity meter, and thermometer, respectively. Also, measuring the alkalinity of thermal water in mmol/l by Aquamerck Alkalinity Test. The second part is the water collection to analyze the concentration of anions, cations, isotopes, and CFC-SF$_6$. In all cases, except the CFC-SF$_6$ sample, the bottle was washed at least three times with sample water to avoid contamination of the sample. The procedure to collect water samples is as follows:

1) Anion analysis: water sample was filtered through a 0.45 μm filter paper with a syringe and stored in a low-density Polyethylene bottle.

2) Cation analysis: water sample was filtered through a 0.45 μm filter paper with a syringe and acidified with 2-3 drops of concentrated hydrochloric acid (HCl) to stabilize various cations in the sample. However, since the analysis uses the pH of the discharge hot spring, the pH measurement was

performed before the sample was acidified. A sample was kept in a low-density Polyethylene bottle.

3) Isotope analysis: Water samples were syringe filtered through 0.45 μm filter paper and stored in brown glass vials to avoid sunlight.

4) CFC-SF$_6$ analysis: A water sample was pumped to fill a glass bottle in a brass container placed in a large bucket. After the brass container is completely covered with water, close the glass plug with a safety clip and close the brass container underwater to avoid air contamination.

All bottles were labelled accordingly, indicating the date, name, and type of the concentration analysis.

2.5 Concentration measurements

All water samples were analyzed at the Institute of Applied Geosciences, Karlsruhe Institute of Technology (Karlsruhe, Germany). The major anion and cation concentrations of all water samples were analyzed in mg/L by Ion Chromatography (IC). Stable isotopes, which are δH and δ^{18}O, were analyzed by the Liquid water isotope analyzer (LWIA). CFC and SF$_6$ are measured by utilizing gas chromatography with an electron capture detector (GC-ECD).

CHAPTER 3
RESULTS

3.1 Hot springs in Southern Thailand

Thirty-three (33) hot springs have been investigated in nine provinces of Southern Thailand. The UTM (zone 47) locations of the hot springs, exit temperatures and pH values are shown in Table 3.1.

Table 3.1 Name and place of investigated Hot springs in 9 provinces of Southern Thailand

Site	UTM (Zone 47)		Temp (°C)	pH	Location	
	East	North			District	Province
ST1	627722	756596	50.0	7.70	Khuan Kalong	Satun
PL1	624763	823636	53.3	7.49	Khao Chaison	Phatthalung
PL2	608623	810397	42.0	8.71	Kong Ra	Phatthalung
PL3	604140	816757	49.6	8.43	Kong Ra	Phatthalung
PL4	615474	859801	41.0	-	Khuan Lhanun	Phatthalung
TR1	551132	819092	48.7	7.11	Kantang	Trang
TR2	573155	803490	48.8	6.54	Pa Lian	Trang
NS1	562482	886069	55.0	-	Bang Khan	Nakhon Si Thammarat
KB1	499549	899932	42.7	7.09	Nuea Khlong	Krabi
KB2	499826	892082	44.6	6.66	Nuea Khlong	Krabi
KB3	509904	888568	45.7	7.00	Khlong Thom	Krabi
KB4	511957	873757	44.5	6.60	Khlong Thom	Krabi
KB5	523171	876867	46.6	6.68	Khlong Thom	Krabi
KB6	522762	865936	36.5	6.89	Khlong Thom	Krabi
SR1	520758	1035200	42.1	7.21	Chaiya	Suratthani
SR2	520214	1034187	40.5	6.90	Chaiya	Suratthani
SR3	522100	1031795	59.1	6.66	Tha Chang	Suratthani
SR4	554753	1009890	40.8	7.44	Kanchanadit	Suratthani
SR5	545450	973281	35.7	7.14	Banna San	Suratthani
SR6	503176	998223	50.4	7.04	Khiri Rat Nikohm	Suratthani
SR7	529068	992240	66.1	6.82	Phun Phin	Suratthani
SR8	530444	991414	56.3	6.60	Ban Na Doem	Suratthani

SR9	524607	977494	58.1	6.83	Khain Sa	Suratthani
PG1	441033	960782	70.0	7.72	Kapong	Phang Nga
PG2	437624	975579	48.9	8.17	Kapong	Phang Nga
PG3	420150	918378	42.5	7.13	Thai Muang	Phang Nga
RN1	461774	1100838	65.0	8.30	Mueang	Ranong
RN2	459670	1095005	40.0	8.30	Mueang	Ranong
RN3	460749	1093805	45.0	8.40	Mueang	Ranong
RN4	462290	1094275	50.0	8.20	Mueang	Ranong
RN5	455853	1080664	46.0	8.30	Mueang	Ranong
RN6	470810	1060430	75.0	8.10	Kapoe	Ranong
RN7	466565	1111520	45.7	7.39	Laun	Ranong
CP1	511994	1075308	47.3	6.78	Lamae	Chumphon

3.2 Geological setting of hot spring sites

Hot springs with a constant flow rate and the highest temperature compared to all within a hot spring system were chosen for water sampling. A total of 17 hot springs were sampled in six provinces in Southern Thailand consisting of:

- 6 hot springs in Krabi (KB1, KB2, KB3, KB4, KB5, and KB6)

- 3 hot springs in Phang Nga (PG1, PG2, and PG3)

- 1 hot spring in Nakhon Si Thammarat (NS1)

- 3 hot springs in Surat Thani (SR3, SR5, and SR9)

- 3 hot springs in Ranong (Rn3, RN5, and RN7)

- 1 hot spring in Chumphon (CP1)

In the following each hot spring will be described briefly.

3.2.1 KB1

KB1 is an abandoned hot spring known as "Ban Huai Yung Tok hot springs" and is in Huai Yung subdistrict, Nuea Khlong, Krabi province which is in the western part of Krabi. There is one hot spring spot that flows out from clay and soil of KB1 in the rubber plantation that discharges to a small canal. Local geological settings around the KB1 are dominated by Quaternary sedimentary and metamorphic rock. In the northeast of the hot spring, igneous mountains appear. Furthermore, limestone and siltstone ridges are around 10 km far from KB1.

Figure 3.1 Outlet of KB1 or Ban Huai Yung Tok hot spring located next to a small canal in the rubber plantation.

3.2.2 KB2

KB2, which is called "Sala Thewada Namron" is located next to the main road from Krabi international airport to Krabi city in Nuea Khlong, Krabi, and about 8 km away from KB1. The hot spring is under the concrete structure as it was developed for tourist purposes. KB2 is close to mangrove forests that connect to the Krabi shoreline on the west side. The hot springs are located in a Quaternary sedimentary area containing gravel, sand, clay, and lateritic soil deposits.

Figure 3.2 Outflow spot of KB2, called Sala Thewada Nam Ron, is covered with a concrete pipe located on the side of the main road.

3.2.3 KB3

KB3 or "Krabi Hot Spring Park" is one of the famous places for tourists. It has four hot spring spots with one big main hot spring. The hot spring park is surrounded by rubber plantations. The area consists primarily of sand, silt, gravel, clay, and rock deposits. On the east side are a sandstone mountain, limestone, and mudstone ridges.

Figure 3.3 Main hot spring of KB3 is in Krabi Hot Spring Park, Khlong Thom district, Krabi.
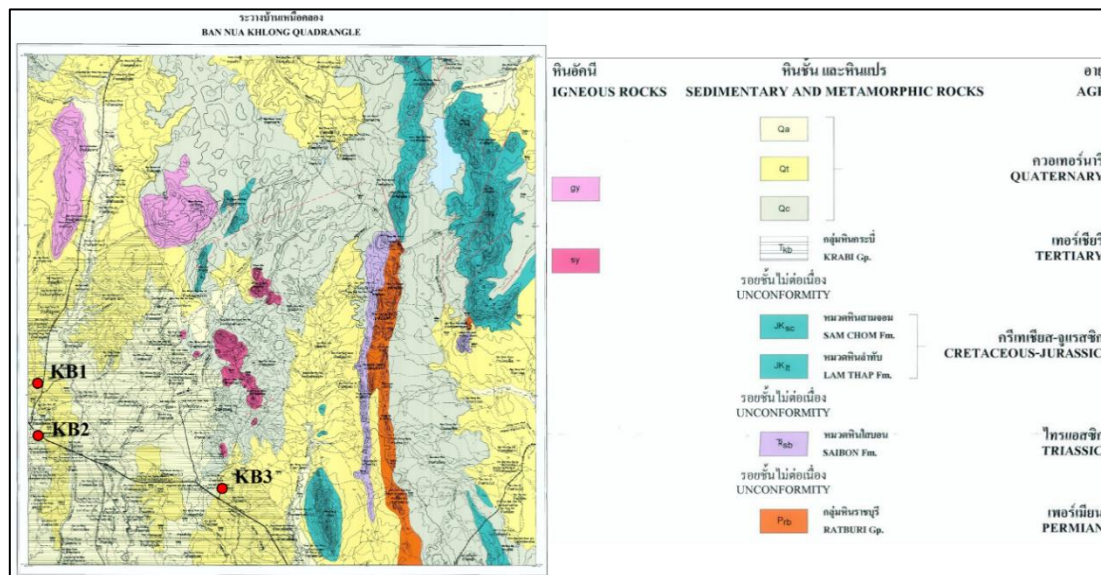
Figure 3.4 Geology map of Ban Nua Khlong Quadrangle, Krabi consisting location of KB1, KB2, and KB3 hot spring.

3.2.4 KB4

KB4 known as Khlong Thom Saline Hot Spring is the most famous hot spring in Krabi located at Huai Nam Khao subdistrict, Khlong Thom district, Krabi. Covering an area of approx.0.5 km^2, there are 15 natural hot springs, 10 in the mangroves, and five outside and nearby. These hot springs are about 5 km away from the Andaman Sea and are connected to a river system that reaches out to the sea. The geology of this area dominantly is nearshore deposits such as clay, sand, plant remain, and shell fragments. Some nearby hot springs of KB4 are covered with limestone rock around the edge. Additionally, sandstone hills and mountains can be found further south and on the east side of the area.

Figure 3.5 KB4 or Khlong Thom Saline Hot Spring

3.2.5 KB5

KB5 hot springs are found in the forest and flow to connect with the waterfall to become the "Krabi hot waterfall" located in Khlong Thom Nuea subdistrict, Khlong Thom district, Krabi. There are around 10 hot spring spots around the area that discharge from a cavity in the land as shown in Figure 3.6. KB5 is surrounded by sandstone hills and mountains, and also a granodiorite outcrop in the southern part.

Figure 3.6 One of discharge hot springs in KB5 found in the jungle. Hot spring water then flows to the waterfall.

3.2.6 KB6

Hot Springs KB6 is located on a locally owned rubber plantation in Krabi's Klong Phong district. At the time of sampling, the hot spring outlet was crushed by a fallen rubber tree. It is covered with red soil along the water stream. In addition, KB6 is located in an area of terraced sediments and near rivers leading to the sea.

Figure 3.7 KB6 hot spring is in a rubber plantation of local people in Khlong Phon subdistrict, Krabi.

Figure 3.8 Geological map of KB4, KB5, KB6, and KBE.

3.2.7 PG1

PG1 Hot Springs is located on the banks of the Pai Phu River. At least five points discharge hot spring water at 70°C into the river. The main site is a pond close to the river with only sediments inside. Rocks around the PG1 are dominantly granite rocks. The geology of these hot springs is a lower Permian-Carboniferous sedimentary rock surrounded by Cretaceous igneous rocks.

Figure 3.9 PG1 main hot spring spot is a big pond next to the Plaipoo canal.
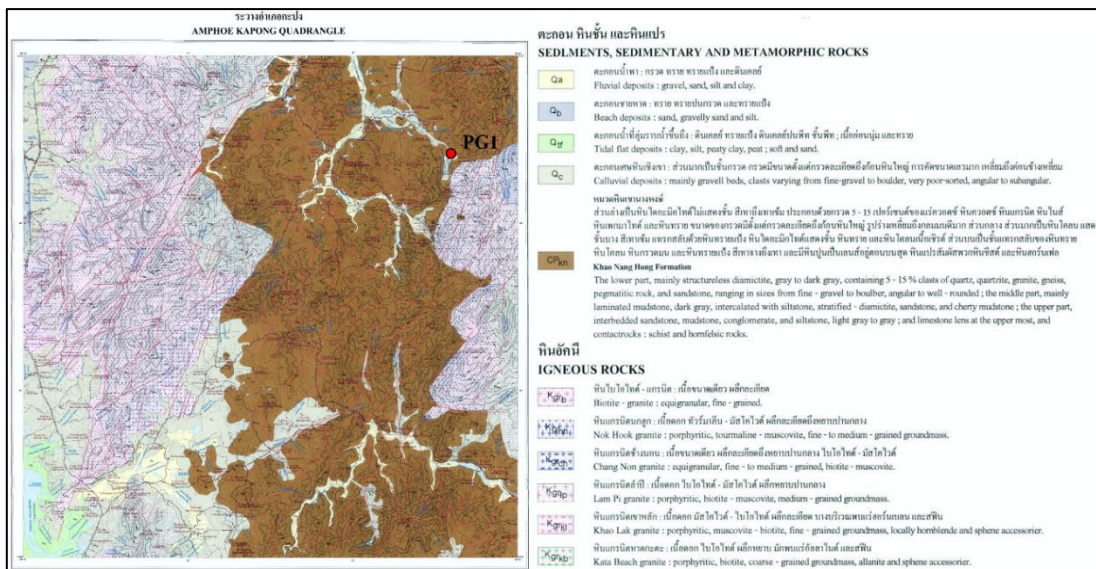
Figure 3.10 Geological map of PG1.

3.2.8 PG2

PG2 or Rommanee Hot spring is a natural hot spring with five hot springs flowing up from underground, occurring on the plains along the watercourse. Rommanee Mountain consists of sandstone and mudstone located in the east of the hot spring. PG2 is also located 20 km away from the Andaman Sea. Granite mountains can be found on the west coast of about 10 km from PG2.

Figure 3.11 Hot springs in PG2 discharge into a canal and some overflow into the mainland.
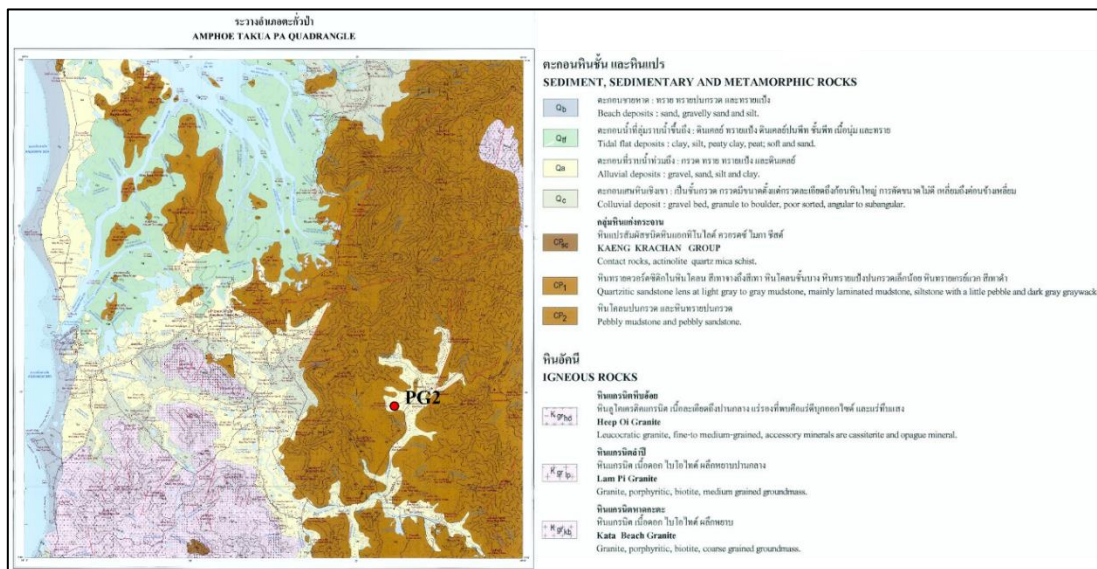
Figure 3.12 Geological map of PG2.

3.2.9 PG3

PG3 is in Bor Dan subdistrict, Thai Muang district, Phang Nga, and is managed by The Hot Spring Beach Resort & Spa Hotel. It is next to the shoreline of the Andaman

Sea. There is one shot spring spot in the area with clearly a distinct red stain on the wall of the pool. The water level varies depending on the time of year. The geology of the area consists mainly of mangrove swamps, alluvial and colluvial deposits. In addition, there are igneous mountains, north-south sandstone ridges, and several limestone outcrops.

Figure 3.13 One main hot spring spot in PG3 connects with a pipe that flows thermal water to a tourist pool.
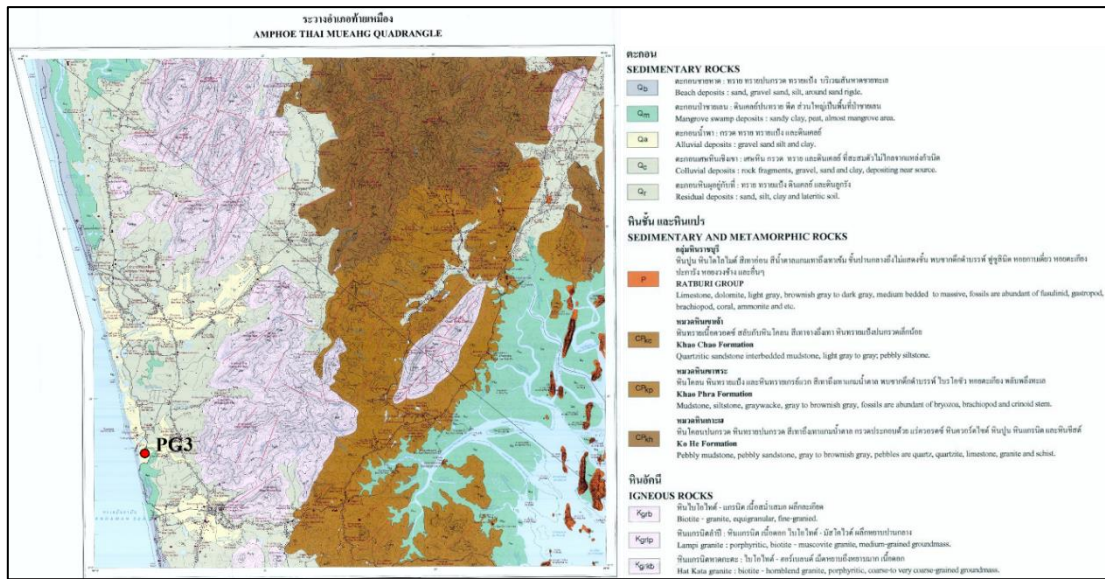
Figure 3.14 Geology map of PG3.

3.2.10 NS1

NS1, known as Ban Khan Hot Springs, is located in Wang Hin Sub-District, Ban Khan District, Nakhon Si Thammarat. The NS1 system has many hot springs, but there are also some hot springs that already dry. The main hot spring flows out into a large area of a large pool surrounded by green algae. The geology around NS1 consists primarily of colluvium and terrace deposits, as well as small dolomitic limestone outcrops found nearby.

Figure 3.15 Main hot spring pool of the NS1 hot spring system.
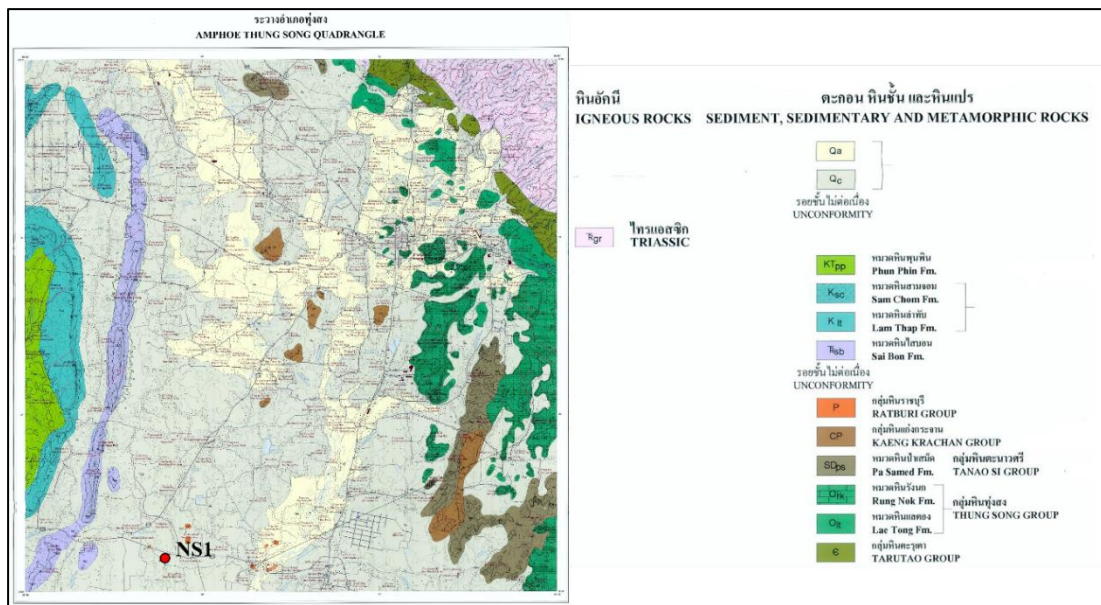
Figure 3.16 Geology map of NS1.

3.2.11 SR3

SR3 or Ban Than Nam Ron is located in the Khao Thanh subdistrict of the Tha Chang district of Surat Thani. The main hot spring is developed to a pool that is piped into the spa pool. However, there is another discharge point nearby, which steady flow out into the river. NS1 is located near the eastern coast of southern Thailand or the Gulf of Thailand. It lies on sandstone mountains surrounded by tidal flat deposits such as gravel, silt, clay, and sand.

Figure 3.17 Hot well spring of SR3 flow to the canal.
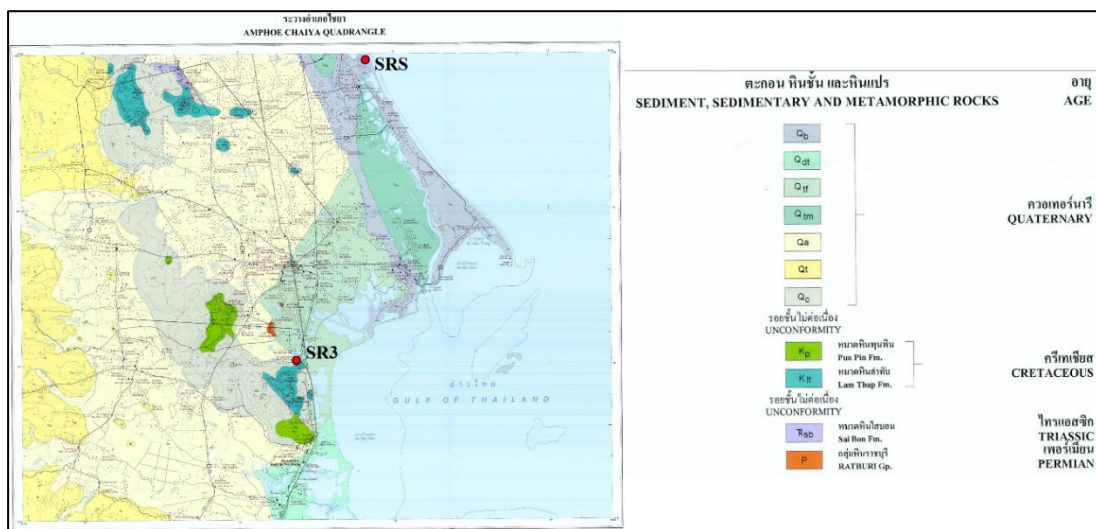
Figure 3.18 Geology of SR3 and SRS (SR Sea).

3.2.12 SR5

Hot Spring SR5 is located at the Scout Camp in Phoem Phun Sap Subdistrict, Ban Na San District, Surat Thani Province. This hot spring is mainly used by locals. There is an old spring nearby, but it no longer discharges. SR5 sits at the foot of sandstone hills with limestone and shale containing mountains on the other side.
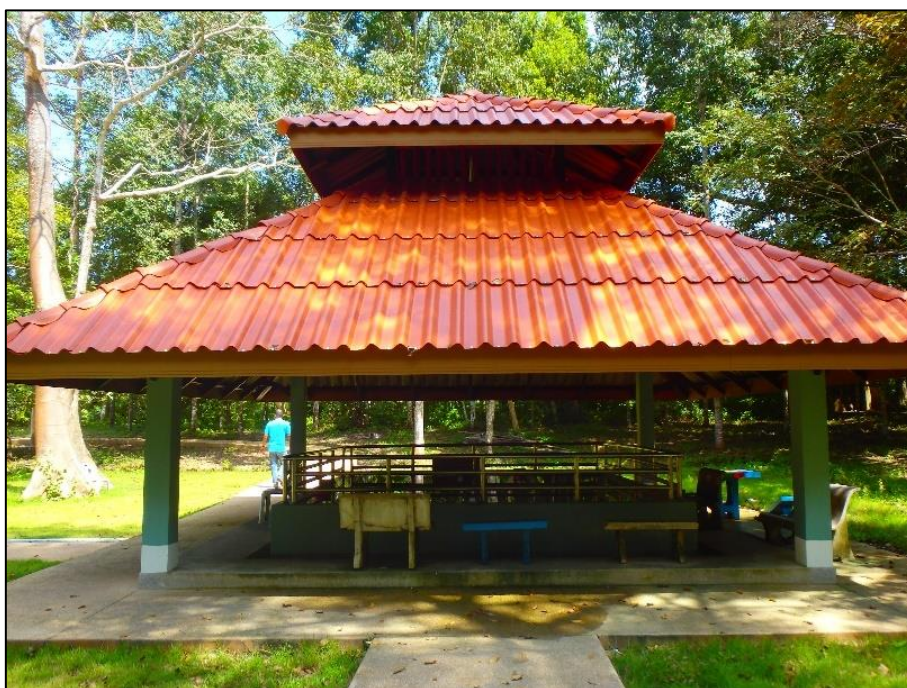
Figure 3.19 SR5 hot spring is developed as a tourist spot.
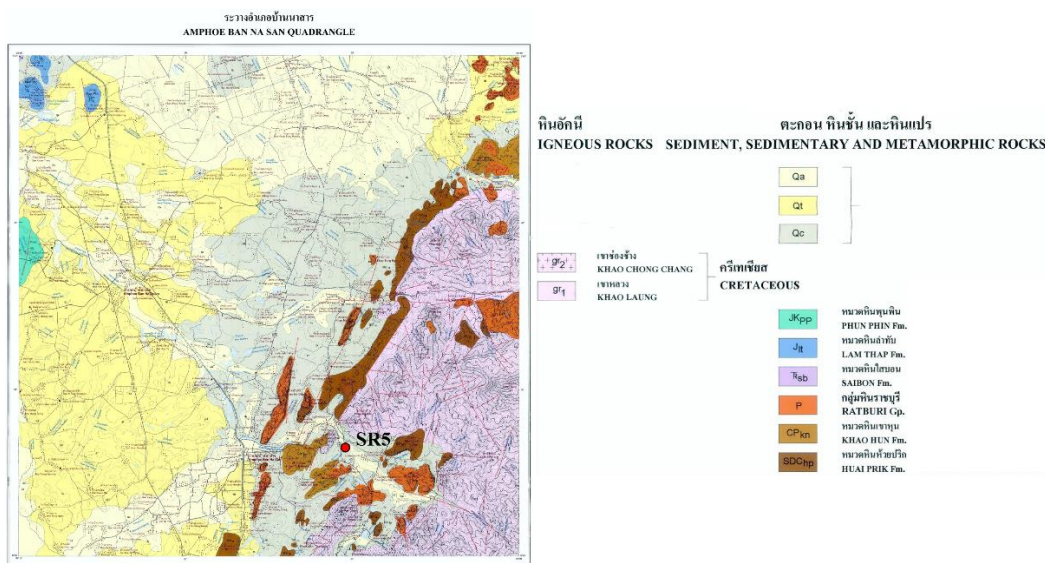
Figure 3.20 Geology map of SR5.

3.2.13 SR9

SR9 in Khian Sa District is located in a national park area. There are about 10 hot springs with a temperature of 60 degrees Celsius in the park. Most hot springs are surrounded by concrete, while others flow directly into the mainland and join rivers downhill. The geology of the national park consists of sandstone and mudstone mountain and clay sediments.

Figure 3.21 Sampling spot in SR9 is at a hot spring that discharges to the surface at a constant rate.

Figure 3.22 Geology of SR9.

3.2.14 RN3

Pornrang Hot Springs or RN3 is located in Bang Rin Subdistrict, Mueang District, Ranong Province, in the area of Ngao Waterfall National Park, around 10 km from the west coast. It is one of Ranong's most famous tourist attractions. Most springs are separated by concrete structures. The hot springs are located in a granite mountain and a mudstone mountain next to it.

Figure 3.23 Hot spring of RN3 is surrounded by concrete structure to separate it from the waterfall.

3.2.15 RN5

RN5 is a hot spring located in the Rattana Rangsan Military camp at Mueang Ranong of Ranong province. RN5 is developed to produce mineral drinking water used in military camp. The hot spring is between the granite ridge that positions along from north to south and the mangrove area.

Figure 3.24 RN5 hot spring well is used to produce mineral drinking water.
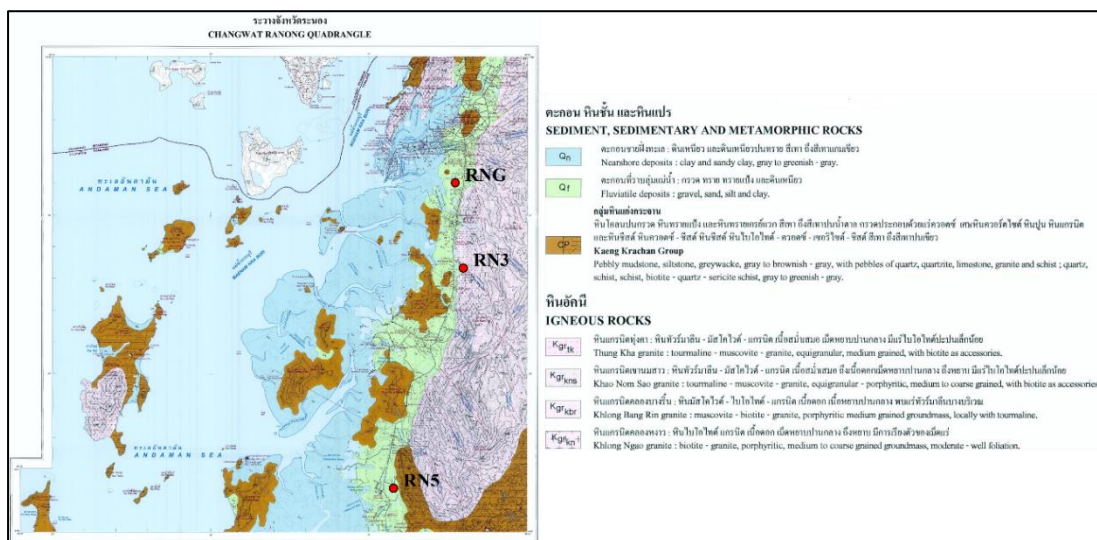
Figure 3.25 Geology of RN3, RN5, and RNG (groundwater).

3.2.16 RN7

RN7, known as Hadyay Hotspring, is located in Laun District, Ranong Province. The hot springs are on the way to the top of the mountain, especially the hot springs flowing out from the crack of the rocks. RN7 is located between sandstone and granite mountains.

Figure 3.26 Main hot spring of RN7 is in the mountain surrounded by small outflow hot spring spots.
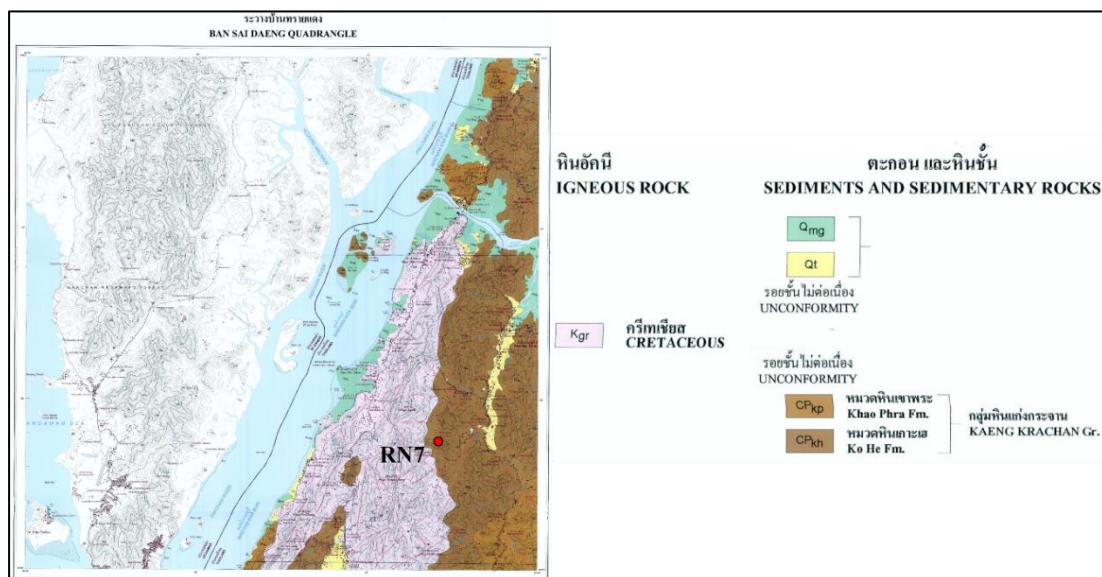
Figure 3.27 Geology map of RN7.

3.2.17 CP1

Thum Khao Plu hot spring or CP1 locates in Lamae district, Chumphon province. There are 4 hot springs, surrounded by dense forests at the foothill of a

limestone mountain. On the sampling day, the carbonate layer was found on the top surface of hot spring water. An area around the site mainly are alluvial and beach deposits.

Figure 3.28 Natural hot spring at CP1 located on the side of Thum Khao Plu hot spring.
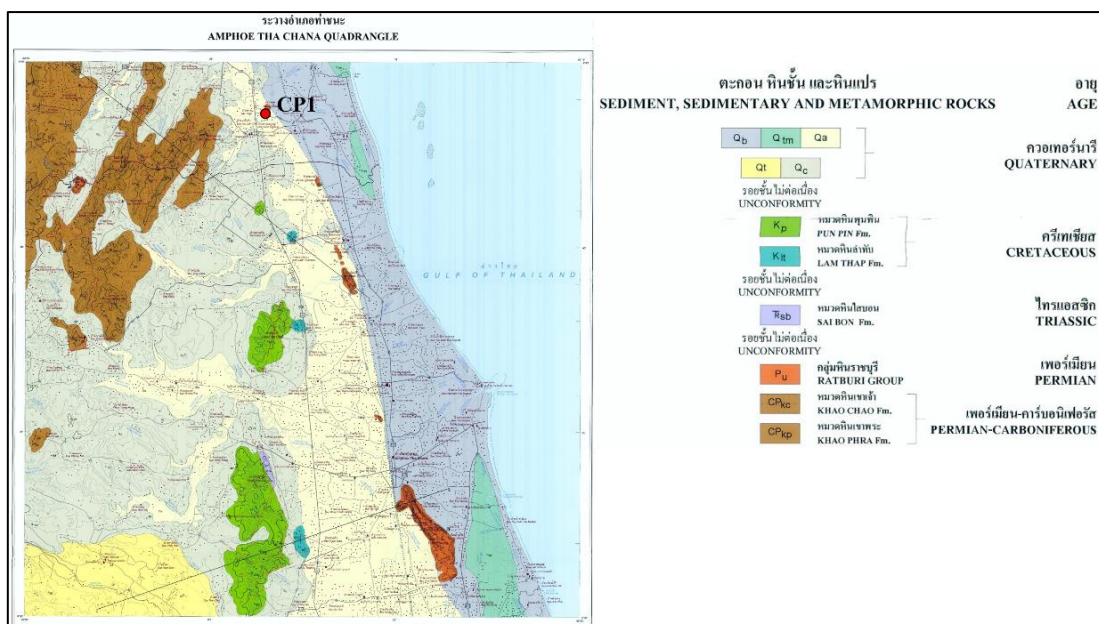
Figure 3.29 Geology of CP1.

In addition, two groundwater samples were collected from village wells in Nuea Khlong district, Krabi (KBG), and in Mueang Ranong district, Ranong (RNG) as shown in Figure3.8 and Figure 3.24 respectively. Two seawater sources were collected along the east coast (Gulf of Thailand) at Krabi estuary (KBE) and the west coast (Andaman Sea) at Surat Thani Sea (SRS). Groundwater and seawater are used as compared parameters of the concentration with the thermal water sample to determine the mix and resources of thermal water in the hot spring system.

3.3 Ion concentration of water samples

The concentration of ions in the water sample was analyzed at the Institute of Applied Geosciences, Karlsruhe Institute of Technology (Karlsruhe, Germany). The surface discharged temperature, pH and significant cations and anions for all water samples are represented in Table 3.2. The discharge surface temperature at the outlet of the source varies from 35°C to 70°C. The average temperature is about 47°C, with the highest temperature at Phang Nga (PG1), followed by SR3 and SR9 at 70°C, 60°C, and 58°C respectively. However, the minimum discharge temperature occurs at SR5 and KB6 at around 36°C. All samples have a pH between 6.6 and 8.2, with a maximum of 8.2 for PG2 and a minimum of 6.60 for KB4. The concentration is in mg/L of major ions including HCO_3^-, F^-, Cl^-, SO_4^{2-}, Na^+, Mg^{2+}, K^+, and Ca^{2+}, obtained from analyzed hot spring samples. A total dissolved solid (TDS) is relatively high in KB2, KB4, and SR3 especially Na and Cl ions, which are around 5,000mg/L and 9,000 mg/L, respectively, are the highest contents compared to others. SO_4^{2-} concentration is also high in SR3 and SR9.

Table 3.2. Discharge temperature, pH, major anion and cation concentrations of water samples from hot spring sites, groundwater wells and seawater.

Site	Temp	pH	Content (mg/L)							
			HCO_3^-	F^-	Cl^-	SO_4^{2-}	Na^+	Mg^{2+}	K^+	Ca^{2+}
KB1	42.7	7.09	329.508	0.28	31.79	5.33	18.07	16.38	2.42	83.22
KB2	44.6	6.66	201.366	n.a.	9176.80	895.22	5044.00	244.80	132.64	1010.80
KB3	45.7	7.00	250.182	n.a.	1877.11	89.36	946.50	69.45	19.96	254.50
KB4	44.5	6.60	207.468	n.a.	9440.01	1395.11	5352.00	325.80	182.90	958.20
KB5	46.6	6.68	317.304	1.16	4.66	268.18	2.57	29.70	1.18	149.50
KB6	36.5	6.89	268.488	1.73	129.76	389.69	37.74	31.60	2.39	229.60
PG1	70.0	7.72	170.856	9.70	3.30	22.07	65.86	0.22	2.64	8.10
PG2	48.9	8.17	164.754	12.96	9.37	69.15	93.88	0.12	3.10	7.33
PG3	42.5	7.13	97.632	n.a.	3016.35	35.07	1278.00	3.37	53.95	709.50
NS1	48.4	7.13	292.896	0.34	3.07	5.10	3.94	13.01	3.11	72.90
SR3	59.1	6.66	170.856	n.a.	6253.21	691.53	3467.00	95.54	111.70	773.00
SR5	35.7	7.14	213.570	7.56	5.17	5.34	63.36	0.33	5.37	16.64
SR9	58.1	6.83	219.672	3.01	6.03	876.08	12.68	38.64	4.46	347.80
RN3	43.6	7.69	140.346	4.78	2.97	44.42	46.46	0.04	3.03	21.61
RN5	40.6	7.94	146.448	4.93	2.84	11.74	40.38	0.05	1.87	19.18
RN7	45.7	7.39	164.754	6.03	2.94	6.79	43.37	0.06	3.15	20.42
CP1	47.3	6.78	457.650	0.37	92.79	12.63	65.28	27.97	6.96	104.90
Groundwater										
KBG	29.4	5.71	48.816	n.a.	9.39	2.99	9.99	2.58	2.71	10.58
RNG	28.8	4.47	n.a.	0.06	3.67	0.29	2.82	0.44	1.78	1.09
Seawater										
KBE	29.4	7.83	140.346	n.a.	15459.95	2233.89	9010.00	1102.50	323.70	391.70
SRS	29.2	7.88	91.530	n.a.	5611.43	816.10	3219.00	383.80	122.20	149.90

Stable isotopes in this study focus on oxygen and hydrogen isotopes precipitated in water. The variations in D/H and $^{18}O/^{16}O$ isotopic ratios are expressed as per mil (‰) deviation with respect to standard mean ocean water (VSMOW) and shown in Table 3.3. The isotopic composition of the thermal sample water has relatively uniform, ranging from -5‰ to -7‰ for oxygen ratio and from -30‰ to -40‰ for hydrogen ratio. However, the ratios in KB2, KB3, and SR3 are slightly below the average of other hot springs.

Table 3.3 Stable isotope ratio expresses as per mil (‰) deviation with respect to standard mean ocean water (VSMOW).

Site	Isotope (VSMOW)	
	$d^{18}O/^{16}O$	$d^2H/^1H$
KB1	-6.40	-40.01
KB2	-3.27	-20.16
KB3	-5.65	-36.32
KB4	-2.75	-18.62
KB5	-6.12	-36.50
KB6	-6.48	-38.82
PG1	-6.01	-35.84
PG2	-5.68	-33.18
PG3	-5.25	-29.48
NS1	-6.26	-39.04
SR3	-3.85	-27.69
SR5	-6.59	-40.98
SR9	-6.22	-41.28
RN3	-5.55	-33.40
RN5	-6.06	-35.37
RN7	-6.02	-33.73
CP1	-7.06	-44.72
Groundwater		
KBG	-5.82	-35.44
RNG	-5.35	-30.64
Seawater		
KBE	-0.82	-5.61
SRS	-2.91	-14.70

The sampling spots for CFC/SF$_6$ measurements should be a hot spring with a constant flow rate being emitted to the atmosphere. These hot springs in this study took place in 10 hot springs including KB1, KB4, PG1, PG2, NS1, SR3, SR5, SR9, RN3, and RN7, and also 1 groundwater at KBG and 1 seawater at KBE. Concentration of CFC in pmol/l, including CFC-11, CFC-12 and CFC-113, and SF$_6$ in fmol/l are shown in Table 3.4

Table 3.4 Location, sampling date, and the concentration of CFC in pmol/l and SF6 in fmol/l.

Sites	Concentration (pmol/l)			SF$_6$ (fmol/l)	Sampling date
	CFC-11	**CFC-12**	**CFC-113**		
KB1	0.27 ± 0.05	0.15 ± 0.05	0.02 ± 0.05	0.3 ± 0.1	29.11.2019
KB4	0.18 ± 0.05	0.11 ± 0.05	0.01 ± 0.05	0.1 ± 0.1	27.11.2019
PG1	0.09 ± 0.05	0.06 ± 0.05	0 ± 0.05	0.3 ± 0.1	01.12.2019
PG2	0.14 ± 0.05	0.08 ± 0.05	0.01 ± 0.05	0.2 ± 0.1	02.12.2019
NS1	0.49 ± 0.05	0.31 ± 0.05	0.03 ± 0.05	0.6 ± 0.1	27.11.2019
SR3	0.27 ± 0.05	0.18 ± 0.05	0.02 ± 0.05	0.4 ± 0.1	04.12.2019
SR5	0.80 ± 0.1	0.47 ± 0.05	0.06 ± 0.05	1.1 ± 0.2	04.12.2019
SR9	0.46 ± 0.05	0.30 ± 0.05	0.03 ± 0.05	0.6 ± 0.1	04.12.2019
RN3	0.44 ± 0.05	0.29 ± 0.05	0.03 ± 0.05	2.9 ± 0.3	06.12.2019
RN7	0.24 ± 0.05	0.17 ± 0.05	0.02 ± 0.05	1.3 ± 0.2	06.12.2019
Groundwater					
KBG	1.7 ± 0.2	1.1 ± 0.1	0.15 ± 005	2.3 ± 0.3	30.11.2019
Seawater					
KBE	1.4 ± 0.2	0.89 ± 0.05	0.08 ± 0.05	1.6 ± 0.2	28.11.2019

3.4 Geochemistry of water samples

The relative concentration of major cations which are Na^+, Ca^{2+}, Mg^{2+}, and K^+, and major anions which are Cl^-, F^-, SO_4^{2-}, CO_3^{2-}, and HCO_3^- were described using the Piper diagram, which is shown in Figure 3.30, by plotting two triangles of corresponding cations concentration and anions concentration then summarize both triangles with one diamond shape.

Based on the position of hot spring samples on the diamond-shaped of Piper's plot, there are four different groups of hot springs: I) KB2, KB3, KB4, PG3, and SR3 fall in the zone of dominant Na and Cl, II) the second group includes PG1, PG2, SR5, RN3, RN5, and RN7 are in the Na and carbonate zone, III) the third group consists of KB1, NS1, and CP1 mix with Ca, Mg, and carbonate concentration, and IV) the last group contains KB5, KB6, and SR9 is dominated by Ca^{2+}, Cl^-, and SO_4^{2-}.

Figure 3.30 Piper diagram showing the different chemical compositions of hot spring samples that line in a diamond shape.

Figure 3.31 shows the relationship between Na^+ concentration and Cl^- concentration. Variation of Na concentration in some hot springs shows a linear relationship with Cl^-, as shown in Figure 3.30. These hot spring groups are KB2, KB3, KB4, PG3, SR3, and KBE (Krabi Estuary), but other hot springs are shifted from this trend.

Figure 3.31 Relationship between Na^+ and Cl^- concentration (mg/L).

The carbonate contribution can be explained by the relationship between Ca^{2+}, Mg^{2+}, HCO_3^-, and SO_4^{2-}. Figure 3.32 shows a plot between $Ca^{2+}+Mg^{2+}$ concentration versus $HCO_3^-+SO_4^{2-}$ concentration with a 1:1 carbonate concentration ratio. From the variations in Figure 3.31, one group of hot springs including KB2, KB4, PG3, and SR3 clearly be seen above the 1:1 ratio line. Another group of hot springs, which are KB1, KB5, KB6, CP1, and NS1 are slightly close to the 1:1 ratio, and the last group, which is PG1, PG2, SR5, RN3, RN5, RN7, is below the 1:1 ratio line. In summary, hot springs can be divided into three groups. The first is above the 1:1 ratio line, the next is plotted close to the 1:1 ratio line, and the last group is below the 1:1 ratio line.

The isotopic composition of water samples is plotted on the relationship between δD and $δ^{18}O$ diagram with the meteoric water baseline for Thailand in Figure 3.33, which was acquired from the following equation:

$$δD = 7.35δ^{18}O + 6.11, \text{ with } R^2 = 0.972 .... (1)$$

The trend and distribution of the δD and δ¹⁸O data for the hot spring samples are not significantly different from values of the Thailand meteoric water line, except for KB2, KB3, SR3, and KBE which have slightly lower than the trend values.

The concentrations of dissolved CFC-11, CFC-12, CFC-113, and SF6 expressed in parts per trillion by volume (pptv) are plotted and compared with model calculations with assumptions of Piston flow, exponential mixing, and binary mixing as shown in Figure 3.34. A comparison of the ratio in CFC versus another is represented in Figure 3.34a – 3.34e consisting of (a) CFC-11 versus CFC-12, (b) CFC-113 versus CFFC-12, (c) CFC-113 versus CFC-11, (d) SF_6 versus CFC-12, and (e) SF_6 versus CFC-11. For CFC concentration, all hot spring samples are plotted near a binary mixing at old age from 1940AD – 1970AD except for groundwater and seawater samples which are plotted further at a younger age. Meanwhile, the SF_6 and CFC ratio of RN3 and RN7 shift to an excess of SF_6.
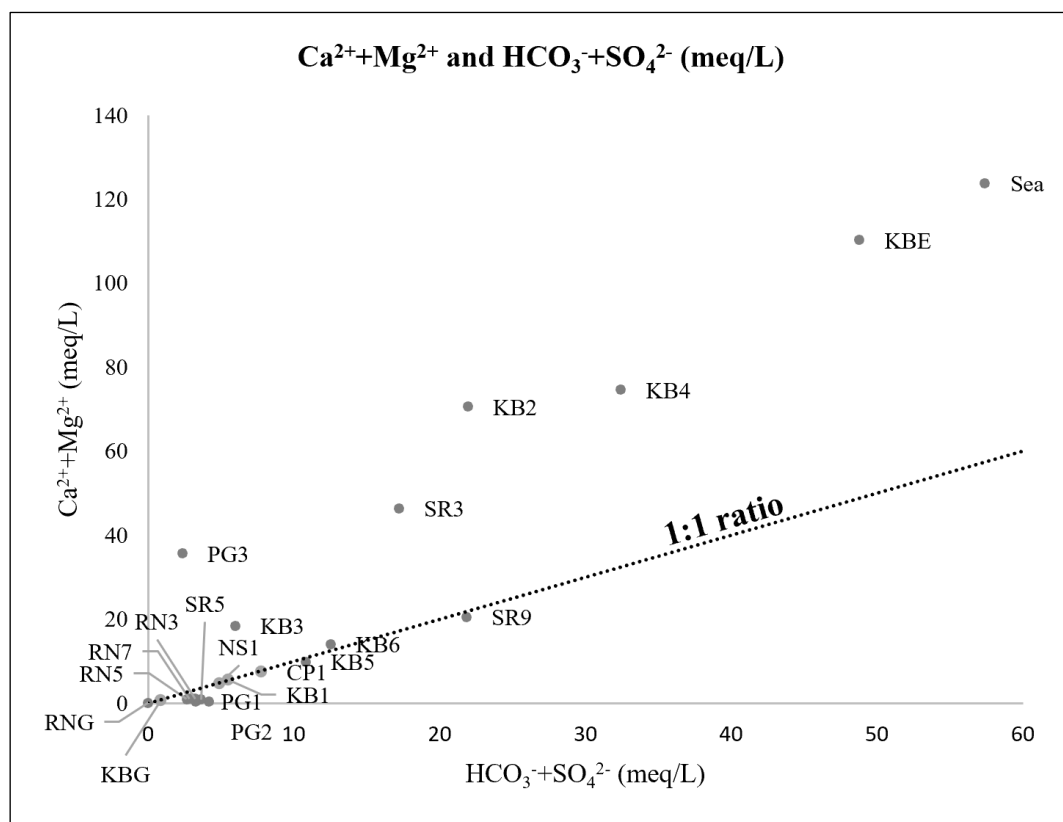
Figure 3.32 Relationship of major carbonate components compared with the 1:1 ratio.
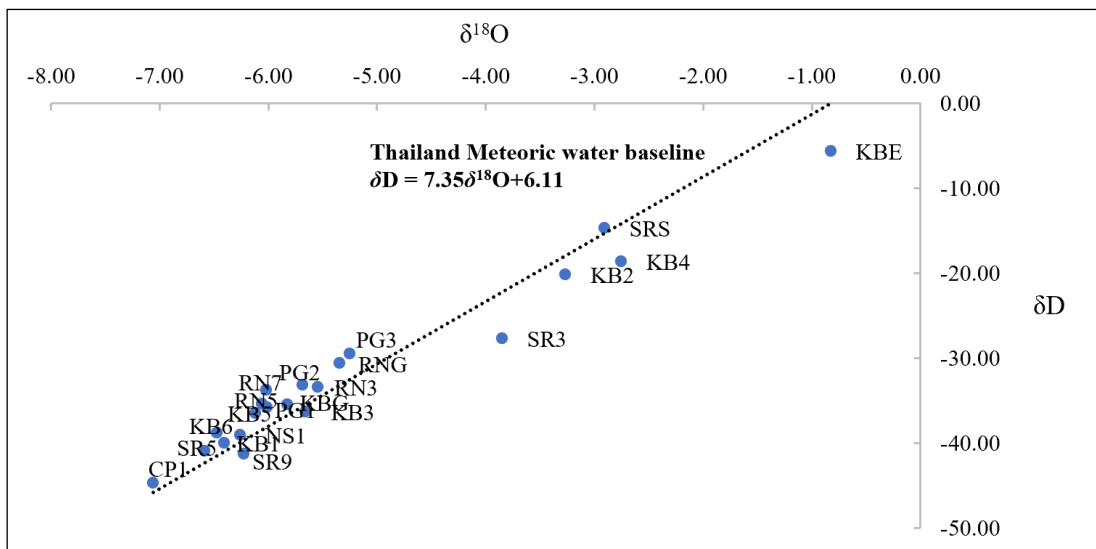
Figure 3.33 Stable isotope of deuterium and oxygen compared with Thailand Meteoric Water Baseline.
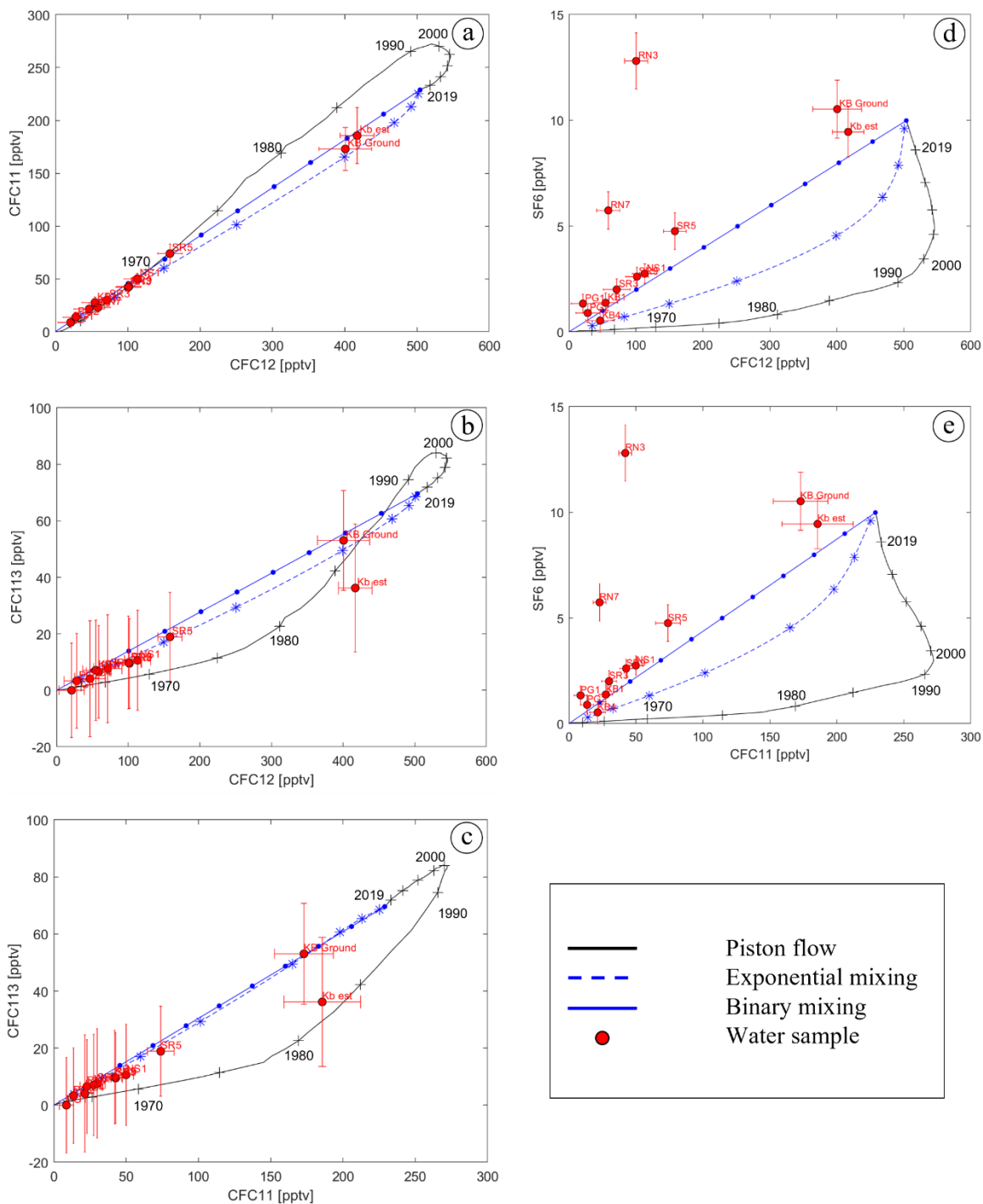
Figure 3.34 Concentrations in pptv plots comparing (a) CFC-11 and CFC-12, (b) CFC-113 and CFC-12, (c) CFC-113 and CFC-11, (d) SF_6 and CFC-12, and (e) SF_6 and CFC-11.

CHAPTER 4

DISCUSSION AND CONCLUSIONS

4.1 Discussion

4.1.1 Thermal water characteristics

The Piper diagram describes the relative concentration of significant cations, which are Na^+, Ca^{2+}, Mg^{2+}, and K^+, and major anions, which are Cl^-, F^-, SO_4^{2-}, CO_3^{2-}, and HCO_3^-. The concentration ratio plots in the two triangles correspond with the cations and anions. The left triangle represents cations, and the right triangle represents anions. The base of the left triangle is calcium (Ca^{2+}), the left is magnesium (Mg^{2+}), and the right is sodium and potassium ($Mg^{2+}+K^+$) axes. For anions, the bottom is the chloride and fluoride (Cl^-+F^-), the left is the carbonate and bicarbonate ($CO_3^{2-}+HCO_3^-$), and the right is the sulfate (SO_4^{2-}) axis. The hydrochemical facies can be identified based on the locations of the hot spring samples on Piper's diamond plot in Figure 4.1, which combines both triangles. This indicates the following four chemical hot springs facies: I) Na^+-Cl^- dominant type including KB2, KB3, KB4, PG3, and SR3, II) Na^+-Mg^{2+}-HCO_3^- type including PG1, PG2, SR5, RN3, RN5, and RN7, III) Ca^{2+}-HCO_3^- type including KB1, NS1, and CP1, and IV) Ca^{2+}-SO_4^{2-} rich type including KB5, KB6, and SR9.

The first group is the Na^+-Cl^- dominated group. Comparing locations with the geology and geography around the hot springs as shown in Figure 4.2, KB2, KB3, KB4, PG3, and SR3 are located near shoreline. High Na^+ and Cl^- ions in water samples are influenced by sea water intrusion.
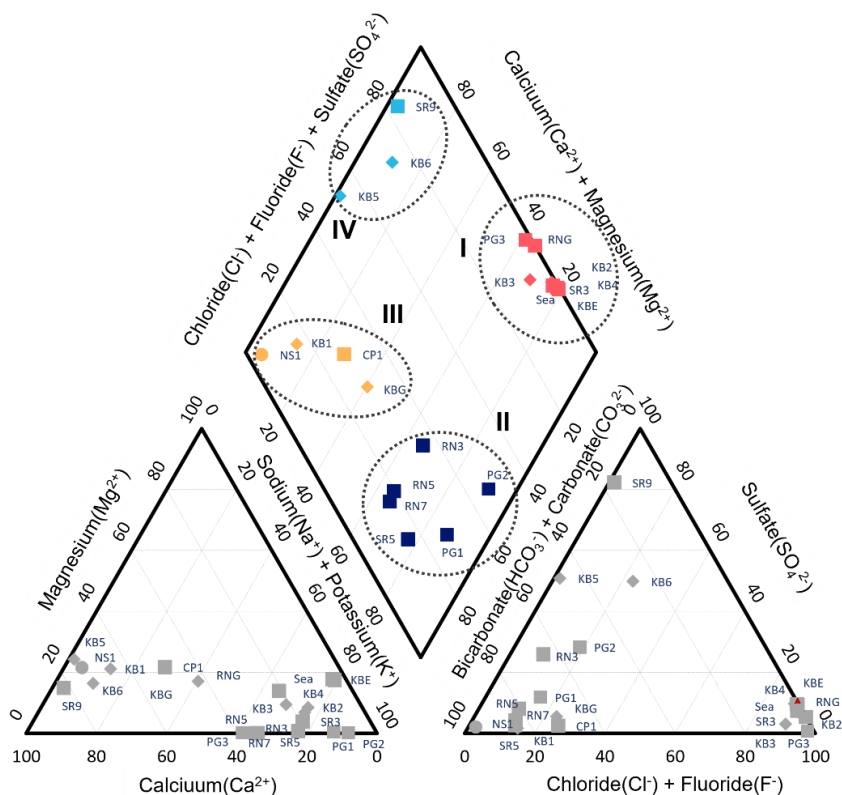
Figure 4.1 Piper diagram showing the chemical composition of hot spring samples. Chemical facies are separated into four types: I) Na^+-Cl^-, II) Na^+-Mg^{2+}-HCO_3^-, III) Ca^{2+}-HCO_3^-, and IV) Ca^{2+}-SO_4^{2-} type.
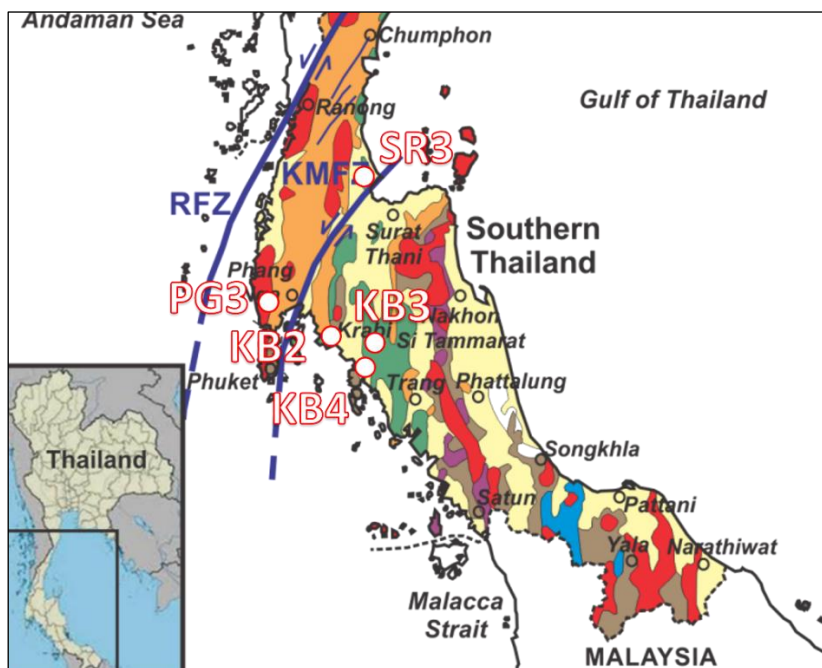
Figure 4.2 Geology map of the hot springs in the Na^+-Cl^- dominated group.

The second is the Na^+-Mg^{2+}-HCO_3^- rich type group. Compared with the geology around the hot springs in Figure 4.3, PG1, PG2, SR5, RN3, RN5, and RN7 locate near igneous area which surrounded with granitic rock (red color in the map). High Na^+ ion in water samples affected by the feldspar from igneous rock.
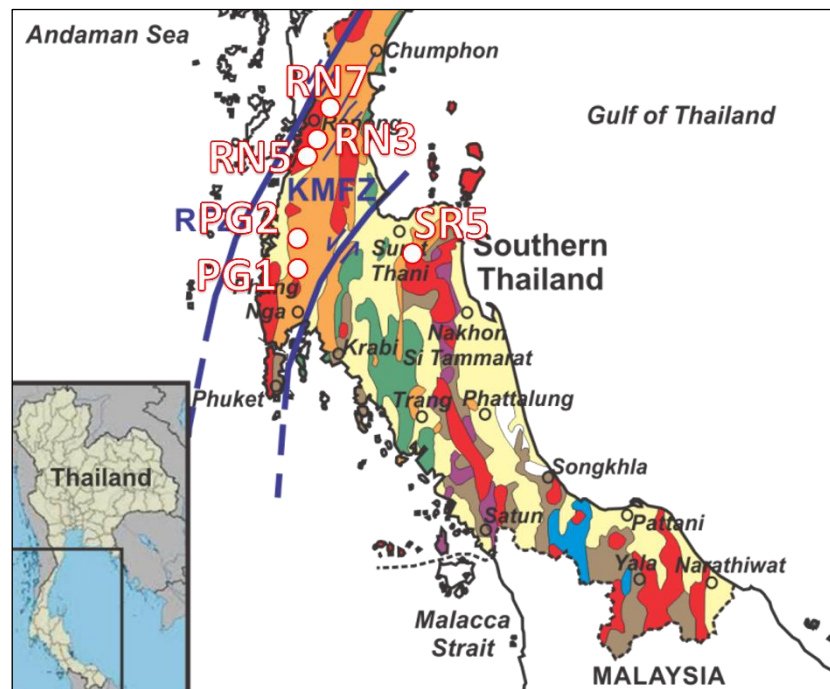
Figure 4.3 Geology map of the hot springs in the Na^+-Mg^{2+}-HCO_3^- rich type.

The third group is Ca^{2+}-HCO_3^- group. Compared with the geology around the hot springs in Figure 4.4, KB1, CP1, and NS1 locate in the sedimentary area (yellow in the map) and surrounding with limestone and sandstone rock. High Ca^{2+} ion in water samples is from limestone and sedimentary deposits.
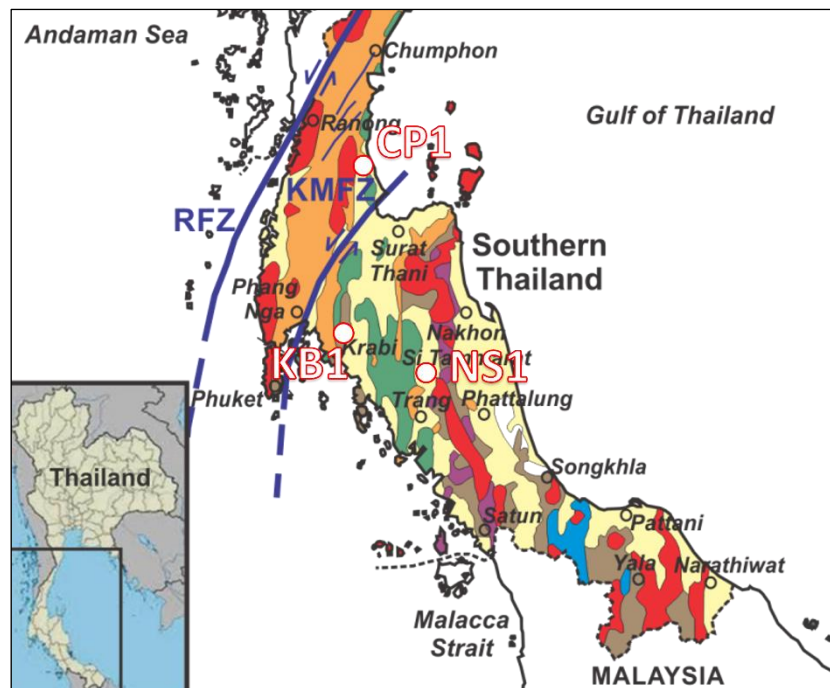
Figure 4.4 Geology map of hot springs in the Ca^{2+}-HCO_3^- group.

The last group is Ca^{2+}-SO_4^{2-} group. Compared with the geology around the hot springs in Figure 4.5, KN5, KB6, and SR9 locate in the sedimentary area which has sedimentary rock and shale outcrop (orange color on the map) close to the sites. Ca^{2+} and SO_4^{2-} ions are from sedimentary deposits and shale rock.
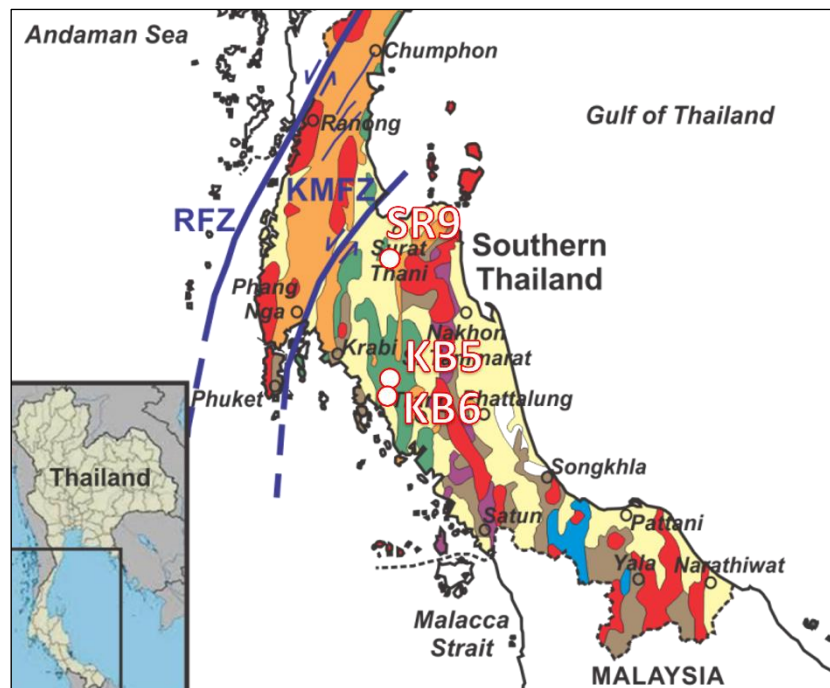
Figure 4.5 Geology map of hot springs in the Ca^{2+}-SO_4^{2-} group.
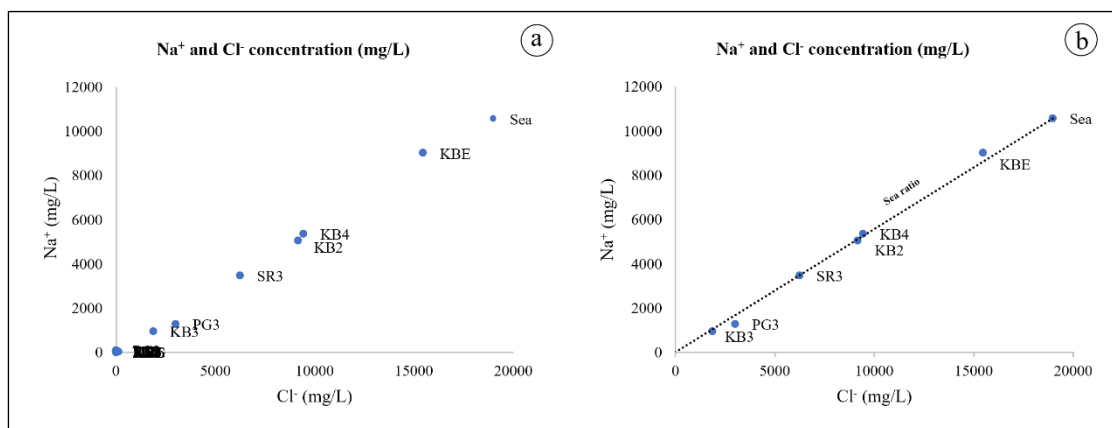
Figure 4.6 (a) Relationship between Na^+ and Cl^- concentration in mg/L, (b) relationship between Na^+ and Cl^- concentration in mg/L with sea ratio.

Na^+ and Cl^- concentrations in milligrams per liter (mg/L) are plotted with Na^+ on the y-axis and Cl^- on the x-axis in Figure 4.6, relative to typical sea ratios. It has been used to identify saltwater intrusion in coastal areas. In Figure 4.6a, there are groups of samples uniquely arranged along the sea ratio. Figure 4.6b focuses on the samples that fall along the sea ratio consisting of KB2, KB3, KB4, PG3, and SR3, as these groups correlate with Na^+-Cl^- rich type according to the chemical facies from the Piper

diagram. Na ions and Cl ions contained in hot springs are affected by seawater mixed with fresh groundwater in the aquifer. The other samples departed from the sea ratio, which can be attributed to other sources of Na^+.
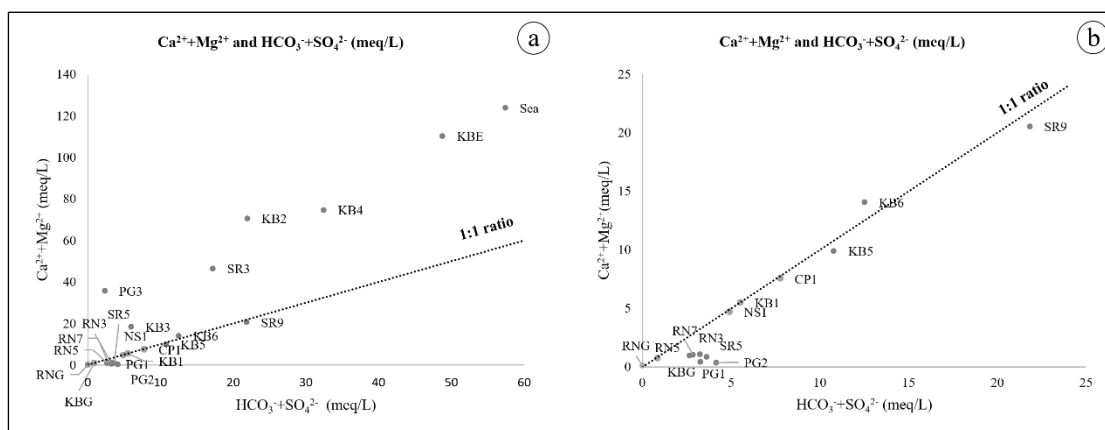
Figure 4.7 (a) Relationship of major carbonate components, and (b) relationship of carbonate components in some hot springs compared with a 1:1 ratio.

The origin of carbonate components in water samples can be explained by the relationship between Ca^{2+}, Mg^{2+}, HCO_3^-, and SO_4^{2-}. Figure 4.7 shows a plot between $Ca^{2+}+Mg^{2+}$ on the y-axis and $HCO_3^-+SO_4^{2-}$ on the x-axis with a 1:1 concentration ratio line. In Figure 4.7a, KB2, KB3, KB4, PG3, and SR3 are well above the 1:1 ratio line, shifting towards excess Ca^{2+} and Mg^{2+}. According to the Piper diagram and Na^+-Cl^- relationship, KB2, KB3, KB4, PG3, and SR3 hot springs have saline intrusion from seawater, hence the excess Ca^{2+} and Mg^{2+} in these hot springs come from the seawater mixture. Figure 4.7b focuses on the other samples except for the seawater mixed group. KB1, KB5, KB6, CP1, and NS1 are hot spring groups plotted near to the 1:1 ratio line which means they have a close relation of Ca^{2+}, Mg^{2+}, HCO_3^-, and SO_4^{2-} as their carbonate components originated from the dissolution of carbonate minerals and dolomite. Dissolved calcium carbonate in water from calcite and dolomite possibly is the main resource for the formation of bicarbonate ions in water. A final group of hot springs, including PG1, PG2, SR5, RN3, RN5, and RN7, showed a slight dominance of $HCO_3^-+SO_4^{2-}$ over $Ca^{2+}+Mg^{2+}$. High concentrations of $HCO_3^-+SO_4^{2-}$ can be a result of the weathering of feldspar and silicate weathering.

4.1.2 Origin of water

The precipitation stable isotope of water samples is described in the relative deviation of hydrogen isotope (δD) over oxygen isotope ($\delta^{18}O$) shown in Figure 4.8. The trend and distribution of the δD and $\delta^{18}O$ data of the hot spring samples are not significantly different from the Thailand meteoric water line which follows the equation $\delta D = 7.35\delta^{18}O + 6.11$ (Kompanart et al., 2004). For the Na^+-Cl^- group, KB2, KB4, and SR3 are different from most of the hot spring trends. This similarity between the hot spring samples and Thailand meteoric water line indicates that the aquifer is recharged from local precipitation and infiltration of meteoric water, predominantly rainwater. Moreover, the difference between other hot springs of the Na^+-Cl^- group is caused by the mixing of seawater in aquifers. Except for PG3 which is in the Na^+-Cl^- group but it was plotted close to other groups of hot springs since PG3 possibly has less proportion of seawater mixing compared to KB2, KB4, and SR3.
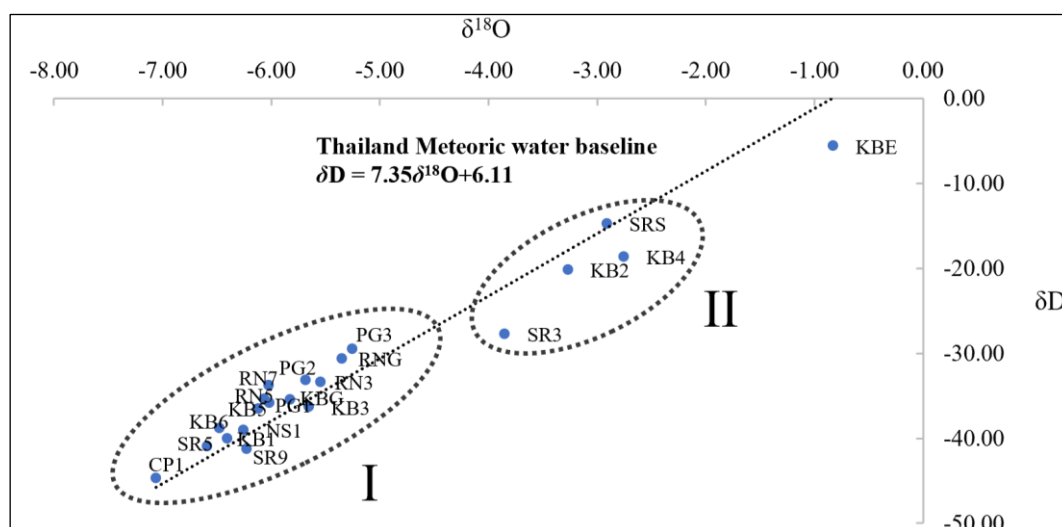
Figure 4.8 The plot of a stable isotope compared with Thailand Meteoric water baseline. (I) Hot springs originally meteoric water recharge, (II) hot springs with seawater mixing.

4.1.3 Age of water

CFC or Chlorofluorocarbon production began in the early 1940s and was used primarily for refrigeration and air conditioning. Until the 1990s when the Montreal Protocol ordered limiting CFC production as CFCs are a factor affecting the ozone

layer, CFC concentration was slightly constant. SF_6 or sulfur hexafluoride was produced in the 1950s for use in electrical and insulation technology and SF_6 concentrations continue to rise. As a result, CFCs and SF_6 were released and dissolved into groundwater at known rates over time shown in Figure 4.9. CFC and SF_6 were used as a groundwater tracer as CFC is only man-made and it can accumulate in water with a long atmospheric lifetime. The release rate of CFC is known from the 1940s to the 1990s. Moreover, the release rate of SF_6 has been known from the 1950s until now therefore the concentration plot of CFC against SF_6 can use to identify the relative age of groundwater.
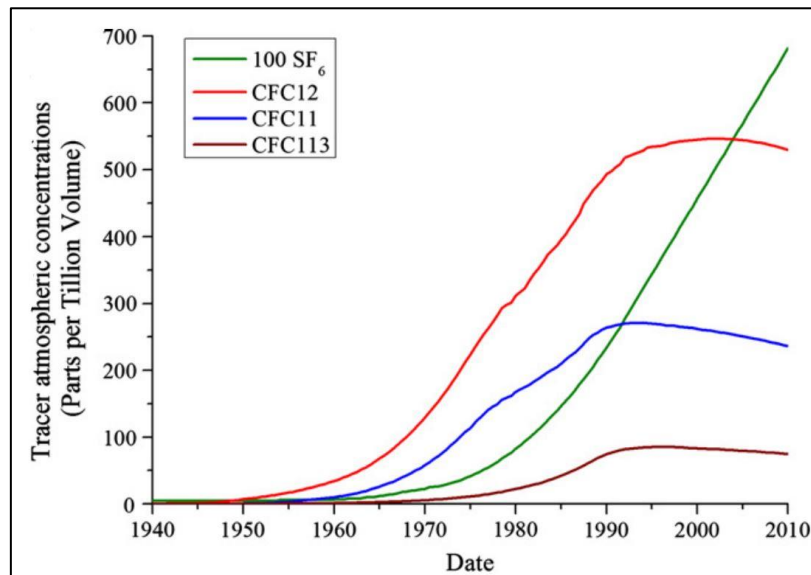
Figure 4.9 Atmospheric concentrations of CFC-11, CFC-12, CFC-113 and 100 SF6 (IAEA, 2006).

In Figure 4.10a to c, CFC concentrations are plotted against each other between CFC-11, CFC-12, and CFC-113 in parts per trillion by volume (pptv) compared with the Piston flow curve, Binary mixing line, and Exponential mixing curve. The piston flow or solid black line represents historical atmospheric concentrations of unmixed recharged water. All hot spring samples, which are KB1, KB4, PG1, PG2, NS1, SR3, SR5, SR9, RN3, and RN7, are plotted close to the binary mixing (blue line) except Krabi estuary and Krabi groundwater samples. The hot spring samples located in the position near old unmixed CFC recharge water indicated that the hot spring samples

were mixed with a high proportion of old reservoir water (before the 1950s) and a low proportion of recharge CFC-accumulated meteorological groundwater (from the 2010s).

In Figure 4.10d and e, SF_6 are plotted against CFC-12 and CFC-11, respectively. Most of hot springs samples are plotted close to the binary mixing except RN3, RN7, and SR5. These hot springs have excess of SF_6 from natural sources since there are no man-made sources around the area of hot spring and F^- concentration in these hot spring samples are relatively high. Compare with the geology in Figure 4.11, these hot springs locate near the igneous area thus the SF_6 likely are from fluorite mineral in igneous rock.
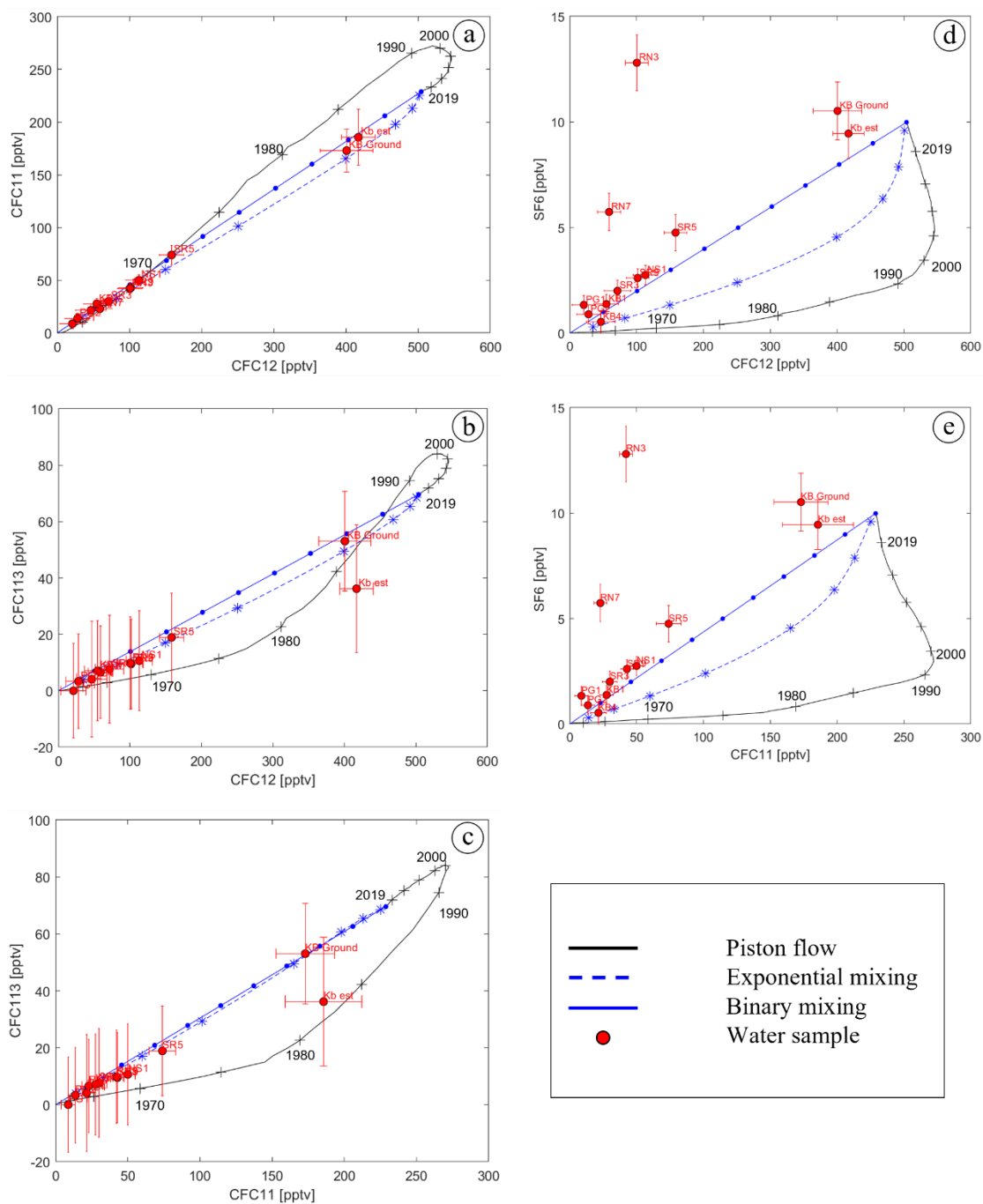
Figure 4.10 Concentration comparing of (a) CFC-11 and CFC-12, (b) CFC-113 and CFC-12, (c) CFC-113 and CFC-11, (d) SF6 and CFC-12, and (e) SF6 and CFC-11 with the Piston flow in black line, the binary mixing in blue line and concentration of selected hot spring samples.
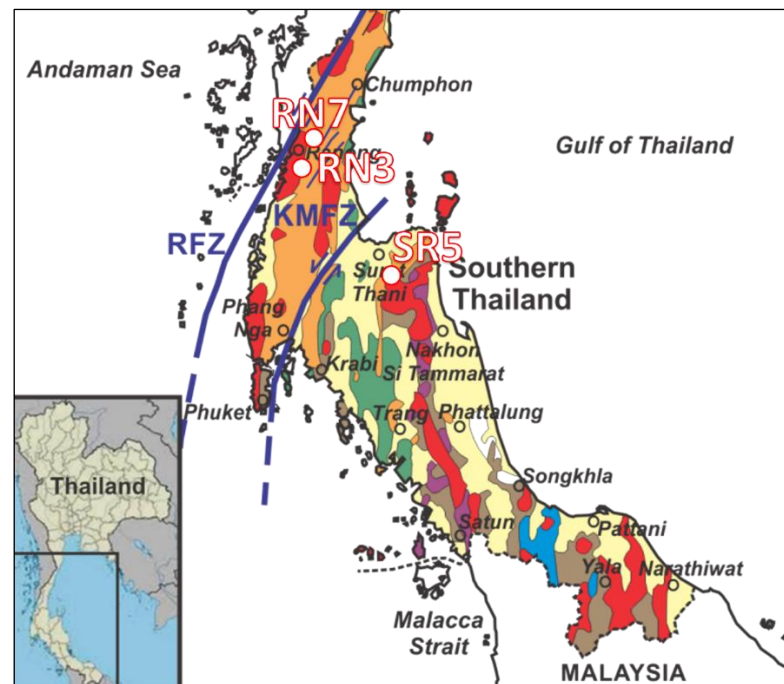
Figure 4.11 Geology map of RN3, RN7, and SR5 which locate near the igneous area (red color).

4.1.4 Geothermal systems in Southern Thailand

Geothermal systems in Thailand can be separated into two main systems shown in Figure 4.12. The first system is the hot spring in igneous area which in most cases find within the Upper Peninsula. Meanwhile, the second one is the hot spring in sedimentary area which commonly position in the Lower Peninsula since there are fault zones (e.g. KMFZ) that cut across the peninsular. Some hot springs close to shoreline are affected by seawater intrusion, although some hot springs are not. The boundary between them can possibly be the different of geological structures, faults, and fractures in subsurface.
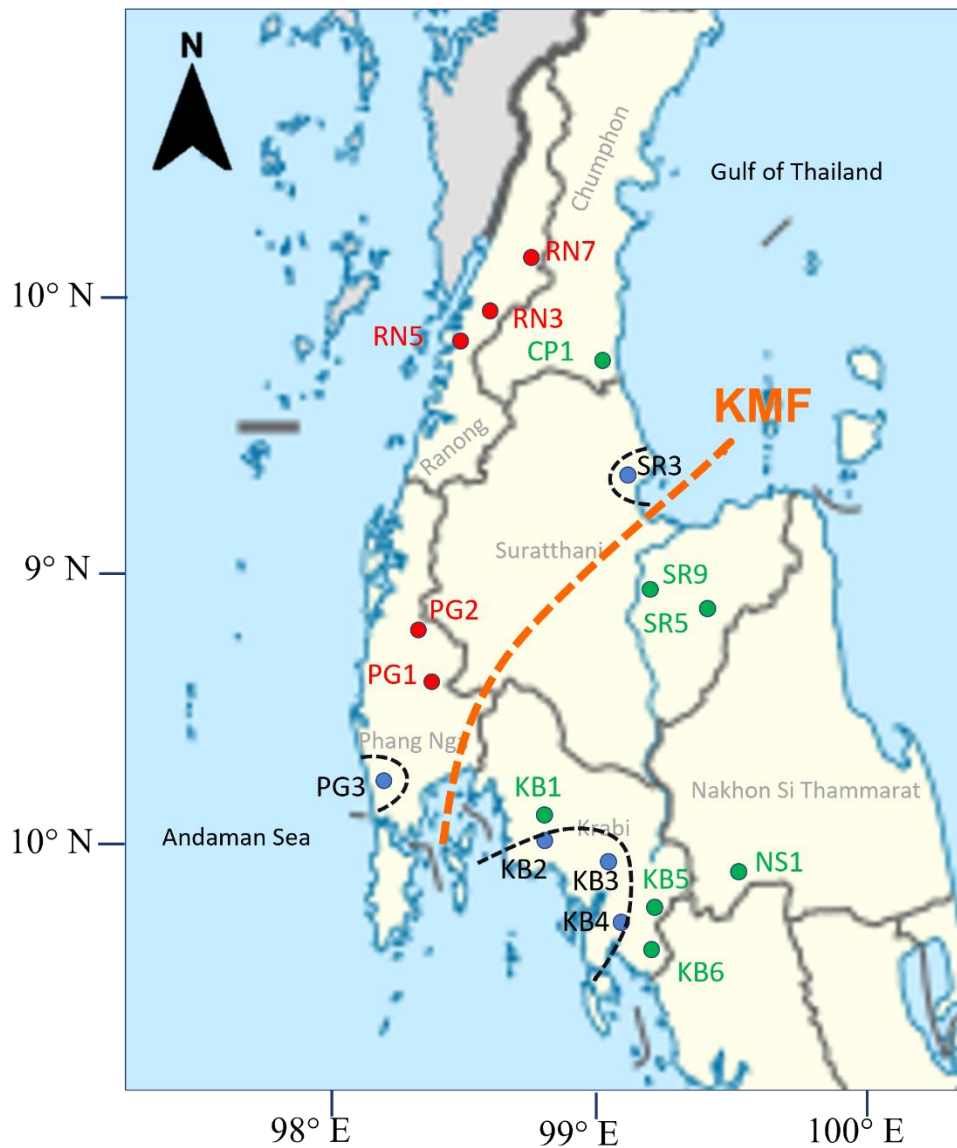
Figure 4.12 Geothermal systems in Southern Thailand: red dot is hot spring in igneous area, green dot is hot spring in sedimentary area, and blue dot is hot spring mixed with seawater.

4.2 Conclusion

Hot springs in Southern Thailand separated into two main systems which are hot spring in igneous area and in sedimentary area and hot springs can be characterized based on chemical composition into ดนีฬ chemical facies type as follow: Na^+-Cl^-, Na^+-Mg^{2+}-HCO_3^-, Ca^{2+}-HCO_3^-, and Ca^{2+}-SO_4^{2-} rich type. Hot springs which locate near

shoreline have seawater intrusion in the aquifer which influenced by different geological structure around the hot spring sites.

The age of hot springs in Southern Thailand is relatively similar. The pathway of geothermal water in Southern Thailand is mainly from old local precipitation water that accumulated in the system before the 1950s and then mixed with low proportion of recharged fresh meteoric water from the 2010s going downwards into the subsurface and heated up by heat sources and finally to be discharged at the subsurface as a hot spring.

REFERENCES

Abdel-halim, A. M., and Aly-eldeen, M. A. (2016). Characteristics of Mediterranean Sea water in vicinity of Sidikerir Region, west of Alexandria, Egypt. The Egyptian Journal of Aquatic Research, 42(2), 133–140.

Alfaro, C., and Wallace, M. (1994). Origin and classification of springs and historical review with current applications. Environment Geology, 24, 112–124.

Alfaro, C., and Wallace, M. (1994). Origin and classification of springs and historical review with current applications. Environmental Geology, 24(2), 112–124.

Anuar, M. N. A., Arifin, M. H., Baioumy, H., and Nawawi, M. (2021). A geochemical comparison between volcanic and non-volcanic hot springs from East Malaysia: Implications for their origin and geothermometry. Journal of Asian Earth Sciences, 217.

Apriani, M., Hadi, W., and Masduqi, A. (2018). Physicochemical Properties of Sea Water and Bittern in Indonesia: Quality Improvement and Potential Resources Utilization for Marine Environmental Sustainability. Journal of Ecological Engineering, 19(3), 1–10.

Aquilina, L., Ladouche, B., Doerfliger, N., Seidel, J. L., Bakalowicz, M., Dupuy, C., and Strat, P. Le. (2002). Origin, evolution and residence time of saline thermal fluids (Balaruc springs, southern France): Implications for fluid transfer across the continental shelf. Chemical Geology, 192, 1–21.

Armannsson, H. (2016). The fluid geochemistry of Icelandic high temperature geothermal areas. Applied Geochemistry, 66, 14–64.

Bersetb, H., and Abdel-Aal, S. I. (1975). Ion exchange removal of calcium carbonate and gypsum from mineral material prior to determination of cation exchange capacity using $^{89}Sr^{++}$. Colloid and Polymer Sci., 253, 322–324.

Beyer, M., Morgenstern, U., Raaij, R. Van Der, and Martindale, H. (2017). Halon-1301 – further evidence of its performance as an age tracer in New Zealand groundwater. Hydrology and Earth System Sciences, 21, 4213–4231.

Bufe, A., Hovius, N., Emberson, R., Rugenstein, J. K. C., Galy, A., Hassenruck-gudipati, H. J., and Chang, J. (2021). Co-variation of silicate, carbonate and sulfide weathering drives CO_2 release with erosion. Nature Geoscience, 14, 211–216.

Cerar, S., and Urbanc, J. (2013). Carbonate Chemistry and Isotope Characteristics of Groundwater of Ljubljansko Polje and Ljubljansko Barje Aquifers in Slovenia. The Scientific World Journal, 2013.

Chaiyat, N., Chaichana, C., and Singharajwarapan, F. S. (2014). Geothermal Energy Potentials and Technologies in Thailand. J Fundam Renewable Energy Appl, 4(2).

Chambers, L. A., Gooddy, D. C., and Binley, A. M. (2019). Use and application of CFC-11, CFC-12, CFC-113 and SF_6 as environmental tracers of groundwater residence time: A review. Geoscience Frontiers, 10(5), 1643–1652.

Charusiri, P., Buenkhuntod, P., Won-in, K., Thayakupt, M., and Niampan, J. (2003). Characteristics of The Chantaburi Thermal Spring, Eastern Thailand. J. Sci. Res. Chula. Univ., 28(I).

Charusiri, P., Chaturongkawanich, S., Takashima, I., Kosuwan, S., Won-in, K., and Cat, N. N. (2000). Application of Geothermal Resources of Thailand, Vietnam, and Myanmar to Tectonic Settings. World Geothermal Congress.

Christopherson, R.W. (2012). Geosystems An introduction to physical geography. United States: Harper Collins.

Cortecci, G., Boschetti, T., Mussi, M., Lameli, C. H., Mucchino, C., and Barbieri, M. (2005). New chemical and original isotopic data on waters from El Tatio geothermal field, northern Chile. Geochemical Journal, 39, 547–571.

Darling, W. G., Gooddy, D. C., Morris, B. L., and Macdonald, A. M. (2010). Using CFCs and SF6 for groundwater dating: A SWOT analysis. Water-Rock Interaction, 13, 15–22.

Dauda, M., and Habib, G. A. (2015). Graphical Techniques of Presentation of Hydro-Chemical Data. Journal of Environment and Earth Science, 5(4), 65–76.

Duriez, A., Marlin, C., Dotsika, E., Massault, M., Noret, A., and Morel, J. L. (2008). Geochemical evidence of seawater intrusion into a coastal geothermal field of central Greece: Example of the Thermopylae system. Environmental Geology, 54(3), 551–564.

Ercit, T. S., Groat, L. A., and Gault, R. A. (2003). Granitic pegmatites of the O'Grady batholith, N.W.T., Canada: A case study of the evolution of the elbaite subtype of rare-element granitic pegmatite. The Canadian Mineralogist, 41, 117–137.

Foster, G. L., Pogge von Strandmann, P. A. E., and Rae, J. W. B. (2010). Boron and magnesium isotopic composition of seawater. Geochemistry Geophysics Geosystems, 11(8).

Ghoddousi, S., Rezaie, B., and Ghandehariun, S. (2021). Guideline for electricity generation from hot springs (natural energy storage systems): A techno-enviro-economic assessment. Sustainable Energy Technologies and Assessments, 47.

Gomez-Diaz, E., and Marin-Ceron, M. I. (2018). Preliminary geochemical study of thermal waters at the Puracé volcano system (South Western Colombia): an approximation for geothermal exploration. Boletin de Geoologia, 40.

Haase, K. B., and Busenberg, E. (2014). Groundwater Dating with Atmospheric Halogenated Compounds. Encyclopedia of Scientific Dating Methods.

Han, D., and Currell, M. J. (2018). Delineating multiple salinization processes in a coastal plain aquifer, northern China: Hydrochemical and isotopic evidence. Hydrology and Earth System Sciences, 22(6), 3473–3491.

Hao, J., Feilberg, K. L., and Shapiro, A. (2020). Kinetics of Calcite Dissolution and Ca − Mg Ion Exchange on the Surfaces of North Sea Chalk Powders. ACS Omega, 5, 17506–17520.

Harnisch, J., and Eisenhauer, A. (1998). Natural CF_4 and SF_6 on Earth. Geophysical Research Letters, 25(13), 2401–2404.

Hartanto, P., Alam, B. Y. C. S. S. S., Lubis, R. F., Ismawan, I., Iskandarsyah, T. Y. W. M., Sendjaja, Y. A., and Hendarmawan, H. (2022). Geothermics The application of hydrogeochemical and stable isotope data to decipher the origin and evolution of hot springs in the Rawadanau Basin, Indonesia. Geothermics, 105.

Held, S., Schill, E., Schneider, J., Nitschke, F., Morata, D., Neumann, T., and Kohl, T. (2018). Geochemical characterization of the geothermal system at Villarrica volcano, Southern Chile; Part 1: Impacts of lithology on the geothermal reservoir. Geothermics, 74, 226–239.

Jankowski, J., and Jacobson, G. (1991). Hydrochemistry of a groundwater-seawater mixing zone, Nauru Island, central Pacific Ocean. BMR Journal of Australian Geology and Geophysics, 12, 51–64.

Jonjana, S., Lohawijarn, W., and Dürrast, H. (2012). Geological structure and origin of the Kaochaison hot spring in Phattalung, Southern Thailand. Songklanakarin J. Sci. Technol., 34(2), 231–239.

Juned A., S., and Arjun B., B. (2011). Analysis of Chloride, Sodium and Potassium in Groundwater Samples of Nanded City in Mahabharata, India. European Journal of Experimental Biology, 1(1), 74–82.

Koh, D. C., Plummer, L. N., Busenberg, E., and Kim, Y. (2007). Evidence for terrigenic SF_6 in groundwater from basaltic aquifers, Jeju Island, Korea: Implications for groundwater dating. Journal of Hydrology, 339, 93–104.

Kraml, M., Jodocy, M., Reinecker, J., Leible, D., Freundt, F., Najem, S. Al, Schmidt, G., Aeschbach, W., and Isenbeck-schroeter, M. (2016). TRACE: Detection of Permeable Deep-Reaching Fault Zone Sections in the Upper Rhine Graben,

Germany, During Low-Budget Isotope-Geochemical Surface Exploration. European Geothermal Congress.

Kumar, P. J. S. (2016). Deciphering the groundwater–saline water interaction in a complex coastal aquifer in South India using statistical and hydrochemical mixing models. Modeling Earth Systems and Environment, 2(4), 1–11.

Kwansirikul, K., Singharajwarapan, F. S., Kita, I., and Takashima, I. (2005). Hydrochemical and Isotopic Characteristics of Groundwater in the Lampang Basin, Northern Thailand. ScienceAsia, 31, 77–86.

Mastrocicco, M., Coolombani, N., and Antonellini, M. (2012). Freshwater-seawater mixing experiments in sand columns. Journal of Hydrology.

Nazaruddin, D. A., and Duerrast, H. (2018). Implication of the 2004 Sumatra-Andaman Earthquake to Seismic Hazards in Southern Thailand. The 7th Asia Conference on Earthquake Engineering, 22–25.

Ngansom, W., and Duerrast, H. (2019). Assessment and Ranking of Hot Springs Sites Representing Geothermal Resources in Southern Thailand using Positive Attitude Factors. Chiang Mai Journal of Science, 46(3), 592–608.

Ngansom, W., Mahapattanathai, P., Maksuwan, A., and Rodphothong, D. (2022). Hydrogeochemical characteristics and terrestrial radiation of geothermal spring attractions in Central and Western Thailand. ScienceAsia, 48(March).

Ngansom, W., Pirarai, K., and Dürrast, H. (2020). Geothermics Geological setting and hydrogeothermal characteristics of the Kapong non- volcanic hot spring area in Southern Thailand. Geothermics, 85.

Nicholson, K. (1993). Geothermal Fluids Chemistry and Exploration Techniques. Germany: Springer-Verlag.

Noor, M., Anuar, A., Hariri, M., Baioumy, H., and Nawawi, M. (2021). Journal of Asian Earth Sciences A geochemical comparison between volcanic and non-volcanic hot springs from East Malaysia: Implications for their origin and geothermometry. Journal of Asian Earth Sciences, 217.

Osman, M., Boschetti, T., Djibril, Y., Baudron, P., Dirir, A., Assowe, O., Mahdi, M., Idriss, S., Ahmed, M., Moussa, N., and Mohamed, J. (2016). Geochemical study of the Sakalol-Harralol geothermal fi eld (Republic of Djibouti): Evidences of a low enthalpy aquifer between Manda-Inakir and Asal rift settings. Journal of Volcanology and Geothermal Research.

Oyuntsetseg, D., Ganchimeg, D., Minjigmaa, A., Ueda, A., and Kusakabe, M. (2015). Isotopic and chemical studies of hot and cold springs in western part of Khangai

Mountain region, Mongolia, for geothermal exploration. Geothermics, 53, 488–497.

Pepin, J., Person, M., Phillips, F., Kelley, S., Timmons, S., Owens, L., Witcher, J., and Gable, C. (2015). Deep fluid circulation within crystalline basement rocks and the role of hydrologic windows in the formation of the Truth or Consequences, New Mexico low-temperature geothermal system. Geofluids, 15, 139–160.

Plummer, L. N., and Busenberg, E. (2006). Chlorofluorocarbons in Aquatic Environments. In Use of Chlorofluorocarbons in Hydrology: A Guidebooks. International Atomic Energy Agency.

Porntepkasemsan, B., Kulsawat, W., and Nochit, P. (2019). Characteristics of the stable isotopes (δ^{18}O and δD) composition in precipitation from Bangkok, KamPhaeng-Phet and Suphanburi, Thailand. KKU Engineering Journal, 43.

Raksaskulwong, M. (2008). Thailand Geothermal Energy: Development History and Current Status. Proceeding of the 8th Asian Geothermal Symposium, 39–46.

Singh, A. K., and Kumar, S. R. (2015). Quality assessment of groundwater for drinking and irrigation use in semi-urban area of Tripura, India. Ecology, Environment and Conservation, 21(1), 97–108.

Singharajwarapan, F. S., Wood, S. H., Prommakorn, N., and Owens, L. (2012). Northern Thailand Geothermal Resources and Development: A Review and 2012 Update. Geothermal Resources Council.

Sonney, R., Vuataz, F. D., and Schill, E. (2012). Hydrothermal circulation systems of the Lavey-les-Bains, Saint-Gervais-les- Bains and Val d'Illiez areas associated with the Aiguilles Rouges Massif in Switzerland and France. Swiss Bull. Angew. Geol., 17/1, 29–47.

Tardani, D., Reich, M., Roulleau, E., Takahata, N., Sano, Y., Pérez-Flores, P., Sánchez-Alfaro, P., Cembrano, J., and Arancibia, G. (2016). Exploring the structural controls on helium, nitrogen and carbon isotope signatures in hydrothermal fluids along an intra-arc fault system. Geochimica et Cosmochimica Acta, 184, 193–211.

Tassi, F., Vaselli, O., Moratti, G., Piccardi, L., Minissale, A., Poreda, R., Delgado Huertas, A., Bendkik, A., Chenakeb, M., and Tedesco, D. (2006). Fluid geochemistry versus tectonic setting: The case study of Morocco. Geological Society London Special Publications, 131–145.

Uchida, Y., Yasukawa, K., Tenma, N., Taguchi, Y., Ishii, T., Suwanlert, J., and Lorphensri, O. (2011). Subsurface Temperature Survey in Thailand for Geothermal Heat Pump Application. J. Geotherm. Res. Soc. Japan, 33(2), 93–98.

Wen, X., Diao, M., Wang, D., and Gao, M. (2012). Hydrochemical characteristics and salinization processes of groundwater in the shallow aquifer of Eastern Laizhou Bay, China. Hydrological Processes, 26(15), 2322–2332.

Wood, S. H., Kaewsomwang, P., and Singharajwarapan, F. S. (2016). Fang Hot Springs Geothermal Area, Chiang Mai Province, Northern Thailand - Geological Geophysical Exploration in 2014-2015. The 11th Asian Geothermal Symposium.

Wu, F. C., Qing, H. R., Wan, G. J., Tang, D. G., Huang, R. G., and Cai, Y. R. (1997). Geochemical of HCO_3^- at The Sediment-Water Interface of Lakes from The Southwestern Chinese Plateau. Water, Air and Soil Pollution, 381–390.

Xia, W., Zhao, X., Zhao, R., and Zhang, X. (2019). Flume Test Simulation and Study of Salt and Fresh Water Mixing Influenced by Tidal Reciprocating Flow. Water, 11.

Zaidi, F. K., Nazzal, Y., Jafri, M. K., Naeem, M., and Ahmed, I. (2015). Reverse ion exchange as a major process controlling the groundwater chemistry in an arid environment: a case study from northwestern Saudi Arabia. Environmental Monitoring and Assessment, 187(10).

Zamora, P. B., Cardenas, M. B., Lloren, R., and Siringan, F. P. (2017). Seawater-groundwater mixing in and fluxes from coastal sediment overlying discrete fresh seepage zones: A modeling study. Journal of Geophysical Research: Oceans, 122, 6565–6582.

Zaporozec, A. (1972). Graphical Interpretation of Water-Quality Data. GROUND WATER, 10(2), 32–43.

Zhao, Z. L. J. (1999). Contribution of carbonate rock weathering to the atmospheric CO2 sink. Environmental Geology, 39, 1053–1058.

Appendix A

Geochemical Signatures of Hot Springs in Southern Thailand

Poonnapa Klamthim [1,2, a)] and Helmut Duerrast [1,2, b)]

[1] *Division of Physical Science, Faculty of Science, Prince of Songkla University, Hat Yai, Thailand.*

[2] *Geophysics Research Center, Faculty of Science, Prince of Songkla University, Hat Yai, Thailand.*

[a)] Corresponding author: aumaimm_pk@hotmail.com
[b)] helmut.j@psu.ac.th

Abstract. Hot springs can be found in most regions of Thailand, from the north to the south, except in the northeast. There are around 120 hot springs altogether, with about 40 hot springs in Southern Thailand, and all are related to non-volcanic geological settings. Most hot springs are mainly developed as tourist destinations, for local as well as for international visitors, often combined with spas or other health-related activities. However, for any further development, including geothermal energy, but not limited to, a better understanding of the relationships between the geological environment and hot water characteristics is required. In this study, field investigations and laboratory measurements were carried out to identify the hydrogeochemical signatures of major hot springs in Southern Thailand, with locations in Krabi, Nakhon Si Thammarat, Phang Nga, Surat Thani, Chumphon, and Ranong Province. Standard and advanced geochemical analysis of water samples was done in laboratories in Thailand and in Germany; samples were collected from natural hot springs, groundwater wells, and seawater sources along the eastern and western coast of Southern Thailand. Results show that the hot springs discharge thermal water with temperatures between 35.7 to 70.0 °C and mostly have an alkaline pH of around 6.6 to 8.1. The major cation and anion concentrations indicate that hot springs in the study area can be classified into four types: Na-Cl, Na-Mg-HCO_3, Ca-HCO_3, and Ca-SO_4 rich type. Carbonate components in the water originated from weathering and dissolution of carbonate and dolomite formations nearby hot springs. Oxygen stable isotope data display a meteoric origin of these thermal waters. Moreover, elevated salinity concentrations (Na, Cl, Mg) in some of the hot springs can be correlated to seawater intrusion from the Andaman Sea in the west or the Gulf of Thailand in the east.

Introduction

A hot spring or geothermal spring is a spring where normal groundwater is geothermally heated by an underground heat source and exiting at the surface as hot water. Most water of such a hot spring system comes from rain that seeps deep into the ground until it reaches an aquifer, thus called groundwater. Such groundwater is heated by hot rocks and rises up through fractures and cracks in the crust and so emerges as a hot spring at the surface. Hot springs can be found in most regions of Thailand, from the north to the south, except in the northeast, which is related to its geological settings [1]. There are around 120 hot springs altogether and about 40 hot springs in Southern Thailand. Most hot springs are mainly developed as tourist destinations combined with health-related activities. Only one hot spring in Northern Thailand is used for electricity production, which is the Fang Hot spring at Chiang Mai. However, for further development, especially in geothermal energy, a better understanding of the relationship between the geological environment and hot water characteristics is required. In this study, field investigations and laboratory measurements were carried out to define the hydrogeochemical signatures of major geothermal systems in Southern Thailand and to identify the influence of groundwater and seawater.

Geology of study area

Southern Thailand sits on a narrow peninsula between the eastern coast, the Gulf of Thailand, and the western coast, the Andaman Sea, and with a political boundary to Malaysia to the south. According to Fig. 1, there are two major fault zones crossing from west to east of the peninsula, first the Ranong Fault Zone and second the Khlong Marui Fault Zone, which cut across further south of the peninsular and separates the upper and lower peninsular. The upper part covers Ranong, Chumphon, Phang Nga, Phuket and the north part of Surat Thani provinces. It mainly consists of Permian shale that lies along Chumphon to Phuket and has intrusion of granitic rocks in some areas. The west coast of the peninsular is a submergent shoreline that predominantly has marine deposits and also colluvial deposits as there is a high mountain range partition between Thailand and Myanmar in the northwest. Limestone and dolomitic limestone also appear in Chumphon, and they are found close to granite bodies in the northwest of Surat Thani. However, the lower part covers Surat Thani to Yala, the southernmost province in Thailand. There are typically Cenozoic sedimentary deposits and sandstones. There is a granite mountain range that extends from Nakhon Si Thammarat to Satun and also some limestone outcrops close to the mountain range. The east coast is an emergent shoreline with a generally marine deposit and clay [2, 3].
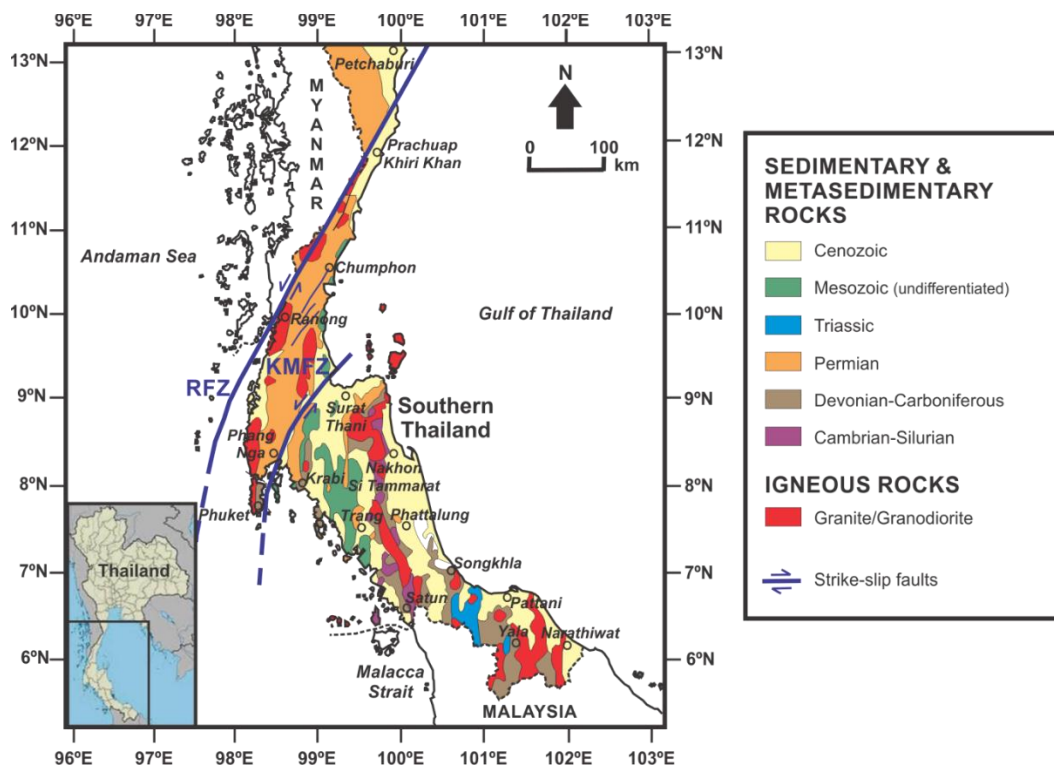
FIGURE 1. General geological map of Southern Thailand
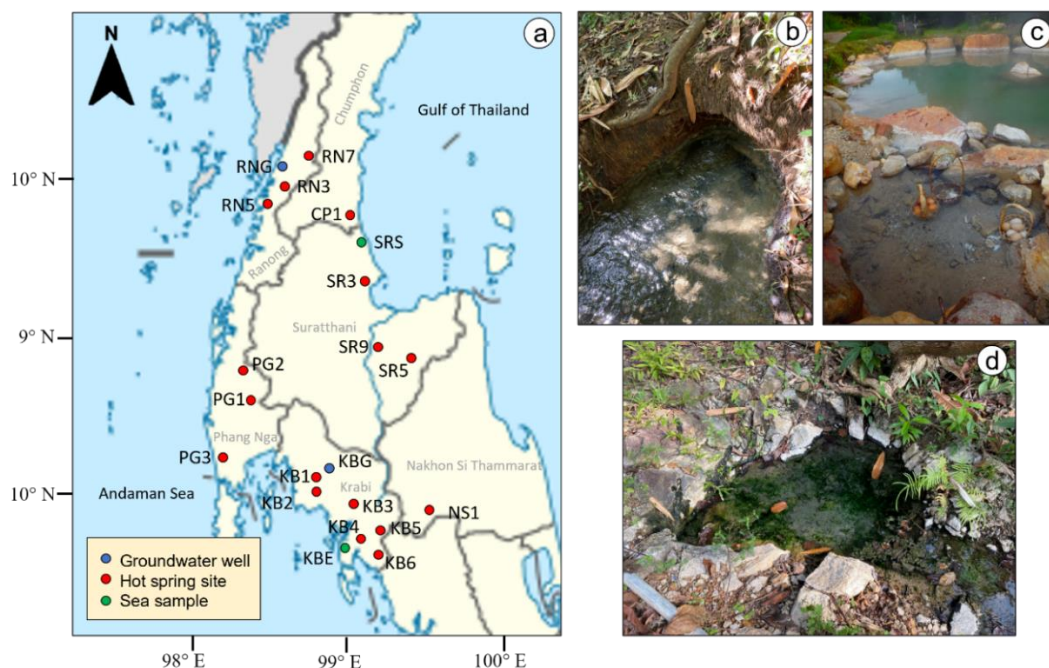
FIGURE 2. (a) Locations of hot spring sites, groundwater wells and sea water samples, (b) Saphanyoong Natural Hot Spring (KB5) at Khlong Thom, Krabi, (c) Rommanee Hot Spring (PG2) at Rommanee, Kapong, Phang Nga, and (d) Hadyay Hotspring (RN7) at Phra Nuea, Laun, Ranong

TABLE 1. UTM locations, discharge temperatures, pH values, concentrations of major anion and cation, and stable isotopes of water sample from hot spring sites, groundwater wells, and seawater samples

Site	UTM (zone 47)		Temp	pH	Content (mg/L)								Isotope (VSMOW)	
	East	North			HCO_3^-	F	Cl	SO_4	Na	Mg	K	Ca	$d^{18}O/^{16}O$	$d^2H/^1H$
KB1	499549	899932	42.7	7.09	329.51	0.28	31.79	5.33	18.07	16.38	2.42	83.22	-6.40	-40.01
KB2	499826	892082	44.6	6.66	201.37	n.a.	9176.80	895.22	5044.00	244.80	132.64	1010.80	-3.27	-20.16
KB3	509904	888568	45.7	7.00	250.18	n.a.	1877.11	89.36	946.50	69.45	19.96	254.50	-5.65	-36.32
KB4	511957	873757	44.5	6.60	207.47	n.a.	9440.01	1395.11	5352.00	325.80	182.90	958.20	-2.75	-18.62
KB5	523171	876867	46.6	6.68	317.30	1.16	4.66	268.18	2.57	29.70	1.18	149.50	-6.12	-36.50
KB6	522762	865936	36.5	6.89	268.49	1.73	129.76	389.69	37.74	31.60	2.39	229.60	-6.48	-38.82
PG1	441033	960782	70.0	7.72	170.85	9.70	3.30	22.07	65.86	0.22	2.64	8.10	-6.01	-35.84
PG2	437624	975579	48.9	8.17	164.75	12.96	9.37	69.15	93.88	0.12	3.10	7.33	-5.68	-33.18
PG3	420150	918378	42.5	7.13	97.63	n.a.	3016.35	35.07	1278.00	3.37	53.95	709.50	-5.25	-29.48
NS1	562482	886069	48.4	7.13	292.90	0.34	3.07	5.10	3.94	13.01	3.11	72.90	-6.26	-39.04
SR3	522100	1031795	59.1	6.66	170.85	n.a.	6253.21	691.53	3467.00	95.54	111.70	773.00	-3.85	-27.69
SR5	545450	973281	35.7	7.14	213.57	7.56	5.17	5.34	63.36	0.33	5.37	16.64	-6.59	-40.98
SR9	524607	977494	58.1	6.83	219.67	3.01	6.03	876.08	12.68	38.64	4.46	347.80	-6.22	-41.28
RN3	460749	1093805	43.6	7.69	140.35	4.78	2.97	44.42	46.46	0.04	3.03	21.61	-5.55	-33.40
RN5	455853	1080664	40.6	7.94	146.45	4.93	2.84	11.74	40.38	0.05	1.87	19.18	-6.06	-35.37
RN7	466565	1111520	45.7	7.39	164.75	6.03	2.94	6.79	43.37	0.06	3.15	20.42	-6.02	-33.73

| CP1 | 511994 | 1075308 | 47.3 | 6.78 | 457.65 | 0.37 | 92.79 | 12.63 | 65.28 | 27.97 | 6.96 | 104.90 | -7.06 | -44.72 |

Groundwater

| KBG | 510334 | 900028 | 29.4 | 5.71 | 48.82 | n.a. | 9.39 | 2.99 | 9.99 | 2.58 | 2.71 | 10.58 | -5.82 | -35.44 |
| RNG | 459677 | 1098452 | 28.8 | 4.47 | n.a. | 0.06 | 3.67 | 0.29 | 2.82 | 0.44 | 1.78 | 1.09 | -5.35 | -30.64 |

Seawater

| KBE | 502982 | 872958 | 29.4 | 7.83 | 140.346 | n.a. | 15459.95 | 2233.89 | 9010.00 | 1102.50 | 323.70 | 391.70 | -0.82 | -5.61 |
| SRS | 522993 | 1058851 | 29.2 | 7.88 | 91.530 | n.a. | 5611.43 | 816.10 | 3219.00 | 383.80 | 122.20 | 149.90 | -2.91 | -14.70 |

Water Sampling

As shown in Fig. 2, altogether 17 thermal water samples were collected in six provinces of Southern Thailand: Krabi (KB), Nakhon Si Thammarat (NS), Phang Nga (PG), Surat Thani (SR), Chumphon (CP), and Ranong (RN). In addition, two groundwater samples were collected in village wells, and two seawater sources were also collected along the eastern (Gulf of Thailand) and western coast (Andaman Sea).

Temperature, pH, conductivity, and alkalinity were measured at the sampling site. Water samples for analysis of major cations and anions were filtered through a 0.45 μm and stored in a low-density polyethylene bottle separately. For cations analysis, samples were acidified using concentrated HCl. Besides, samples for analysis of stable isotope components were filtered and stored in a brown glass bottle. All chemical analyses and stable isotopes were measured in the Institute of Applied Geosciences, Karlsruhe Institute of Technology (Karlsruhe, Germany). All chemical components and isotopic data are shown in Table 1.

Hydrogeochemical analysis and discussions

Locations of hot springs, exit temperatures, pH values, chemical, and isotopic compositions of the water samples are presented in Table 1. The discharge of surface temperature at the spring outlet varies from 35 to 70 °C. The average temperature is around 47 degree Celsius, and the highest temperature is at Phang Nga (PG1), followed by SR3 and SR9 with approximately 58 °C. Although, the lowest discharge temperature takes place at SR5 and KB6 at around 36 °C. pH values range from 6.6 to 8.2, highest is 8.2 at PG2. The concentration in mg/L of major ions including Cl, SO_4, Na, Mg, K and Ca, obtained from analyzed hot spring samples, are relatively high in KB2, 4, PG2, and SR3 compared to other hot springs.

The relative concentration of major cations which are Na, Ca, Mg, and K and major anions which are Cl, F, SO_4 and HCO_3 were described using the Piper diagram to classify a water sample facies group [4-9] by plotting two triangles corresponding with the cations and anion and one diamond that summarize both triangles. Based on the position of hot spring samples on the diamond-shaped of Piper's plot in Fig. 3, there are four different groups of hot springs: I) hot springs fall in the zone of dominant Na and Cl, II) second group is in the Na and carbonate zone, III) the third group consists of mixed Ca, Mg, and carbonate, and IV) the last one is dominated by Ca, Cl, and SO_4. In short, this indicates following four chemical hot springs facies: I) Na-Cl, II) Na-Mg-HCO_3, III) Ca-HCO_3, and IV) Ca-SO_4 rich type.
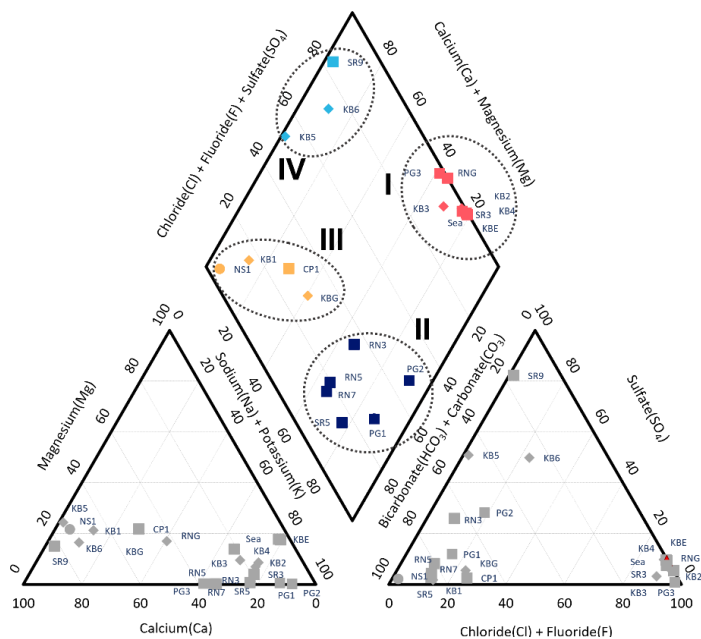
FIGURE 3. Piper diagram showing the chemical composition of hot spring samples. Chemical facies are separated into four types: I) Na-Cl, II) Na-Mg-HCO₃, III) Ca-HCO₃, and IV) Ca-SO₄ type
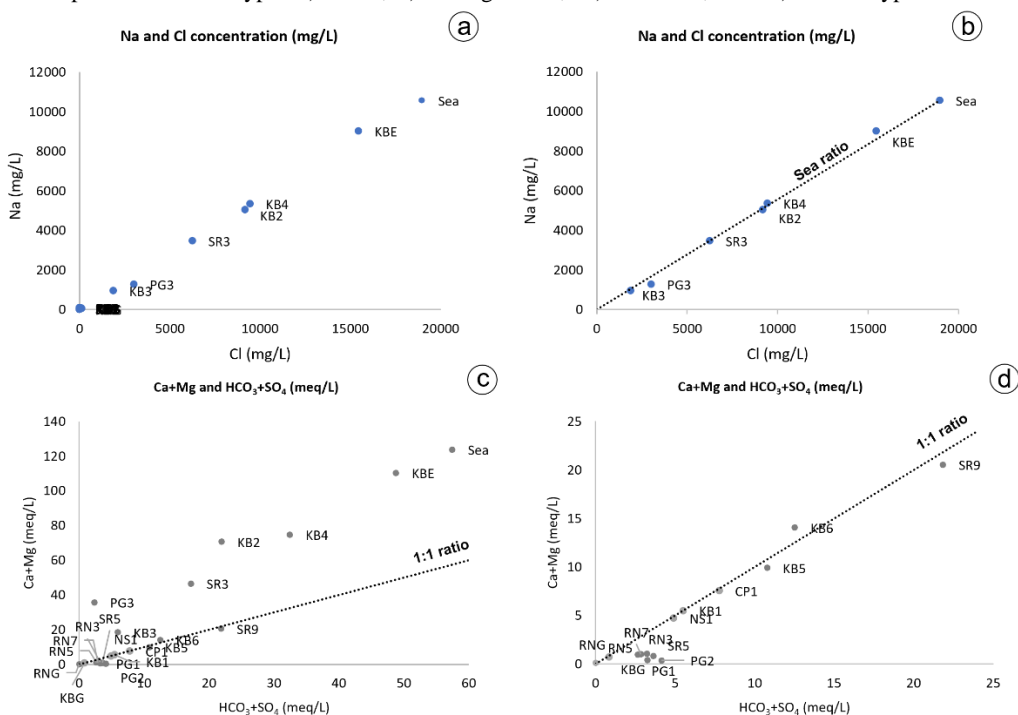
FIGURE 4. (a) Relationship between Na and Cl concentration in mg/L, (b) relationship between Na and Cl concentration in mg/L with sea ratio, (c) relationship of major carbonate components, and (d) relationship of carbonate components compared with 1:1 ratio

The relationship between Na and Cl concentrations is shown in Fig. 4a and b. It is used to identify the influence of saline water in a coastal region. Concentrations of Na in some hot springs show a linear relationship with Cl as shown in Fig. 4a. Compared with the sea ratio in Fig. 4b, KB2, 3, 4, PG3, and SR3, which are Na-Cl rich type according to the Piper diagram, fall along the sea ratio indicating the influence of seawater mixing in an aquifer [10]. Other hot spring sites shifted from the trend, which means that their Na content can be from other sources of Na [11-12].

Carbonate contribution can be described in terms of the relation between Ca, Mg, HCO_3, and SO_4. Figure 4c shows the plot between Ca+Mg against HCO_3+SO_4 with the 1:1 ratio line. Hot springs can be divided into three groups: first is KB2, KB3, PG3, and SR3, which are above the 1:1 ratio line, next are KB1, KB5, KB6, CP1, NS1, and SR9, which are plotted close to the 1:1 ratio line, and the last group is PG1, PG2, SR5, and RN3, RN5, RN7 which are below the 1:1 ratio line. The first group is shifted to the excess Ca and Mg as it has saline intrusion from seawater. Figure 4d displays only the relation between carbonate of the second and the third group to target these groups. The group of hot springs that plotted close to the 1:1 line indicates the origin of carbonate from the dissolution of carbonate minerals and dolomite since there are dolomitic limestone outcrops in such areas. Other hot springs are shifted to an excess of HCO_3+SO_4 showing that their carbonate originated from feldspar and silicate weathering [4, 11, 13].
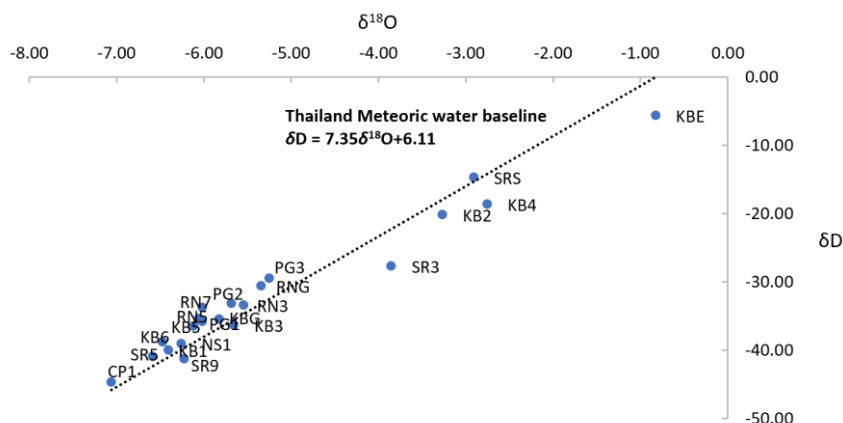
FIGURE 5. Stable isotope of deuterium and oxygen compared with Thailand Meteoric Water Baseline

The variations in D/H and ^{18}O/^{16}O isotopic ratios are expressed as per mil (‰) deviation with respect to standard mean ocean water (VSMOW). The isotopic composition of water samples is plotted on the δD and $\delta^{18}O$ diagram with the meteoric water baseline for Thailand (Fig. 5), which was acquired from the following equation [14]:

$$\delta D = 7.35\delta^{18}O + 6.11, with\ R^2 = 0.972 \tag{1}$$

The trend and distribution of the δH and $\delta^{18}O$ data for the hot spring samples are not significantly different from the Thailand meteoric water line except for the Na-Cl group which has slightly lower than the trend values because of the seawater mixing. A similarity can be interpreted that the hot spring water was recharged from local precipitation and infiltration of meteoric water, predominately rainwater due to the geographic proximity.

CONCLUSION

Hot springs in Southern Thailand can be classified into four types: Na-Cl, Na-Mg-HCO_3, Ca-HCO_3, and Ca-SO_4 rich type. The Na-Cl rich group of hot springs includes KB2, KB3, KB4, PG3, and SR3, which are affected by the seawater mixing with the groundwater. The Na-Mg-HCO_3 rich group contains PG1, PG2, RN3, RN5, RN7, and SR5. Their carbonate originated from the weathering of feldspar and silicate. The third group, Ca-HCO_3 rich, contains KB1, CP1 and NS1. The excess of Ca comes from the dissolution of carbonates such as dolomite in the area. The last one consists of KB5, KB6, and SR9, which have high Ca and SO_4 components. Their SO_4 components derive from the dissolution of limestone. The oxygen stable isotope displays a meteoric origin of thermal water which reveals that the main pathway of geothermal water in Southern Thailand is from local precipitation going downwards into the subsurface and heated up and finally to be discharged at the subsurface as a hot spring.

Acknowledgements

References

1. C. Charusiri, S. Chaturongawanich, I. Takashima, S. Kosiwan, K. Won-in, and N. Cat, The World Geothermal Congress, Tohoku, Japan, 2000, pp. 1043-1047.
2. D. A. Nazaruddin, "Seismicity of Southern Thailand and Peninsular Malaysia," Ph.D. thesis, Prince of Songkla University, 2021.
3. W. Ngansom and H. Durrast, Chiang Mai J. Sci., 46(3), 592-608 (2019).
4. F. K. Zaidi, Y. Nazzal, M.K. Jafri, M. Naeem and I. Ahmed, Environmental Monitoring and Assessment, 187, 10 (2015).
5. M. Awaleh, T. Boschetti, Y. Soubaneh, P. Baudron, A. Kawalieh, O. Dabar, M. Ahmed, S. Ahmed, M. Daoud, N. Egueh and J. Mohamed, Journal of Volcanology and Geothermal Research, 331, p. 26-52 (2017).
6. S. Elzien, S. Mohamed, K. Keiralla, O. Attaj, and H. Hussein, J Geol Geosci 3: 138 (2013).
7. D. Han and M. Currell, Hydrol. Earth Syst. Sci., 22, p. 3473-3491 (2018).
8. J. Jankowski and G. Jacobson, BMR Journal of Australian Geology & Geophysics, 12, p. 51-64 (1991).
9. W. Ngansom, P. Mahapattanathai, A. Maksuwan and D. Rodphothong, ScienceAsia, 48 (2022)
10. X. Wen, M. Diao, D. Wang and M. Gao, Hydrological Processes, 26(15), 2322–2332 (2012).
11. P. J. S. Kumar, Modeling Earth Systems and Environment, 2(4), 1–11 (2016).
12. A. Duriez, C. Marlin, E. Dotsika, M. Massault, A. Noret and J.L. Morel, Environmental Geology, 54(3), 551–564 (2008).
13. D. Oyuntsetseg, D. Ganchimeg, A. Minjigmaa and A. Ueda, Geothermics,53, 488–497 (2015).
14. K. Kwansirikul, F. Singharajwarapan, I. Kita and I. Takashima, Science Asia, 31, 77-86 (2005).

Delineation of Unconventional Groundwater: I. Soda Groundwater in Songkhla, Thailand

Poonnapa Klamthim[1,a], Helmut Duerrast[1,b] and Manussawee Hengsuwan[2,c]

Abstract The majority of groundwater bodies are of conventional type, but in rare cases unconventional groundwater can be found, mainly related to fluids rising from the depth. Soda rich groundwater is a special case of groundwater, called carbon dioxide-rich groundwater or CO_2-rich groundwater. This type of water can be often found in volcanic geological settings, but it is less common in basin settings. Sources of the carbon dioxide vary from site to site. In Thailand there is one known site of soda-rich groundwater, in Khlong Hoi Khong, Songkhla Province. Various geophysical and geochemical methods have been applied to understand and characterize the occurrence and pathways of the CO_2 in this area. Initial results of this ongoing study suggest upper mantle CO_2 as the source and the carbon dioxide moved up along faults before accumulating in shallow groundwater aquifers, which were sealed by clay formations.

Keywords *carbon dioxide, soda-rich groundwater, Southern Thailand, Songkhla*

[1]Geophysics, Department of Physics,
Prince of Songkla University
Hat Yai, Thailand
[2]Department of Groundwater Resources
Ladyao, Chatuchak
Bangkok, Thailand

[a]aumaimm_pk@hotmail.com
[b]helmut.j@psu.ac.th
[c]manussawee.h@dgr.mail.go.th

Introduction

Groundwater is freshwater from rain that is stored under the Earth's surface in pore spaces. The majority of groundwater bodies are of conventional type and its utilization is important for people's livelihood as well as for agriculture and industrial production. In rare cases unconventional groundwater can be found, mainly related to fluids rising from the depth. Soda groundwater is a special case of groundwater, called carbon dioxide-rich groundwater or CO_2-rich groundwater that can occur in special tectonic settings [1]. There is no formal definition of carbon dioxide-rich groundwater, but common characteristics are: slightly acidic, relatively high content of total dissolved solids or TDS, very high partial pressure of carbon dioxide gas in equilibrium with water or $P(CO_2)$, and high concentrations of carbon dioxide fluid which compose of CO_2, HCO_3^- and CO_3^{2-} [2]. Groundwater with high carbon dioxide concentrations is globally distributed but it is not a common phenomenon. A suitable geological system for carbon dioxide storage and carbon dioxide-rich groundwater as shown in Fig. 1 includes: (1) A source of carbon dioxide gas, (2) pathways for carbon dioxide to move from the source upwards into the groundwater, (3) porosity and permeability of the formation that can provide storage volume for the carbon dioxide, and (4) the system must be covered by an impermeable layer acting as a seal to prevent carbon dioxide leakage [3]. Soda groundwater sites can be classified in different geology settings: Volcanic, metamorphic, and sedimentary basin setting. Comparing to the first two settings soda groundwater occurrence in sedimentary basins is less common and also the source of carbon dioxide is not obvious.


Fig. 1. Schematic drawing of the CO_2 pathway from various sources to be accumulated in groundwater becoming CO_2-rich groundwater.

There are many possible sources of CO_2 in groundwater. First is CO_2 from magmatic CO_2 which dissolved in magma as magmatic fluid rises from the upper mantle towards the crust. CO_2 rich mantle fluid moves up along faults or fracture. Second is metamorphic source. The contact metamorphism occurs around magma in high temperature area when magma rises through the rock and interacts with limestone. Third is CO_2 from a decomposition of organic matter or soil organic matter. Last is CO_2 from the weathering of carbonate rock. Carbonic acid from dissolve carbon dioxide in rain water interacts with carbonate rock and then the reaction produces CO_2 in form of calcium bicarbonate [2].

There is one report about CO_2 rich groundwater in Thailand which is located in Khlong Hoi Khong, Songkhla, in Southern Thailand. A better understanding of this soda rich groundwater, which is the objective of this ongoing study, will benefit the people living in the area and might also open opportunities to utilize this unconventional groundwater.

Study area

The study area is in Khlong Hoi Khong at a Royal Research Farm, which is located about 20 km southwest of Hat Yai City, Songkhla Province, Thailand. Many agricultural activities are carried out on this 1.28 km2 farm, e.g. cattle production, fruit tree plantations, and plant crop production. The study area is located in the central part of Hat Yai Basin (Fig. 2 and 3).
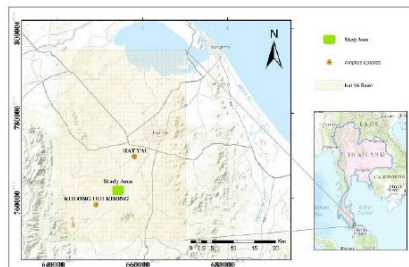
Fig. 2. Topographic map of Hat Yai Basin, Songkhla Province, Thailand (modified after ESRI world topographic map).

Hat Yai Basin is thought to be a graben which is bounded at the east and west by mountain ranges, which are part of a horst system. U-Tapao is the main river system in this area, which is about 80 km long and flows from south to north into the Songkhla Lake. Hat Yai Basin is a sedimentary basin ranging in age from Carboniferous to Quaternary (see Fig 4, next page). Granitic rocks intruded into Carboniferous and Triassic sedimentary rocks. Metamorphic rocks were found mainly at the eastern and western side of the basin, which form the basement of the basin Pegmanite, aplite, and quartz veins locally cut granites and sedimentary rocks. Carboniferous rocks are composed of sandstone, mudstone, chert, and quarzitic sandstone. Triassic rock comprises of a red bed of conglomerates, sandstones, mudstones, and limestone. Late Triassic to early Jurassic granites are mainly coarse-grained porphyritic biotite and biotite-muscovite granites with quartz veins [4].

Hat Yai basin is overlain by thick Quaternary deposits with an age from 1.6 million years to present time. The Quaternary alluvium composes of gravel, sand silt, and clay. The aquifer system comprises of unconsolidated and consolidated aquifers. There are three main aquifers in Hat Yai Basin. The upper aquifer (Hat Yai aquifer) is an unconfined to semi-confined aquifer at a depth of 20 to 40 m. This aquifer consists of moderately to well-sorted sand and gravel and is separated from the lower aquifer by a layer of low permeable clay. The lower aquifer (Khu Tao aquifer) is a confined aquifer, which consists of poorly sorted sand, gravel and several clay layers. The depth to the top of aquifer ranges from 50 to 100 m. The deepest aquifer is the Khohong aquifer, which is deeper than 100 m. It consists of unconsolidated and semi-consolidated clay, sand, and gravel [5].

Drilling encountered at two sites on the Royal Research Farm area soda rich groundwater with well D2 and D4 (see Fig. 3). Only about 500 m north of the well D2 several wells were drilled showing normal (freshwater type) groundwater; well D1 and D9 are shown in Fig. 3.

Methodology

In order to characterize the source and pathways of the soda rich groundwater mainly geophysical and geochemical methods were applied.
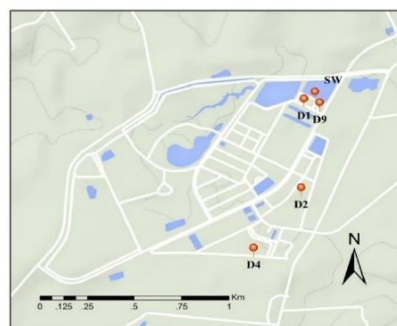
Fig. 3. Sample locations on the Royal Farm: D1 and D9 are non-CO_2-rich groundwater; D2 and D4 are CO_2-rich groundwater locations; SW is surface water. Modified after Google Maps.

Geophysical methods comprise mainly of 1D (vertical electrical sounding, VES) and 2D resistivity surveys (electrical resistivity tomography, ERT) on the farm and in the surrounding area in order to investigate lithological boundaries and fluid pathways in the upper 150 m. Schlumberger configuration was used for VES surveys with maximal AB/2 of 600 m. ERT surveys were conducted in dipole-dipole array type arrangement with maximal n=8. For all measurements ABEM terrameter SAS 1000 was utilized.

To obtain hydrochemical and isotopic data, two samples of CO2-rich groundwater (D2, D4), two samples of non CO2-rich groundwater (D1, D9), one surface water sample, and four borehole cutting samples from a newly drilled groundwater borehole (D9) were collected. D1, D2, D4, and D9 are at 108, 128, 136, and 78 meter depth, respectively (Fig. 3).

All water samples for major cations, rare earth elements and Sr-isotope measurements were filtered through a 0.45 μm membrane filter and acidified to pH 2 with concentrated double-distilled HNO3. Non-acidified water samples were collected for anion and Tritium (3H) determination. For 13C measurement, NaOH was added to water samples to pH 11. Precipitates of BaCO3 formed after adding BaCl2 to the alkaline solution. These precipitates were removed from the residual water and oven-dried at 60 °C.

Fig. 4. Geological map of the larger study area of southern the southern part of Songkhla Province (from and modified after [6]). Red dot – location of farm.

Major cations and anions were performed at the Central Equipment Division, Faculty of Science, Prince of Songkla University (PSU, Thailand) using an ICP-OES, ion chromatography and titration method. Rare earth elements and 13C were analyzed by ICP-MS on a VG Plasma Quad II and Thermo Kiel IV with Finnigan DeltaPlus Mass Spectrometer, respectively, at the Geoscience Centre at University of Göttingen

(GZG, Germany). ^{3}H contents were analyzed by Liquid Scintillation Counter (Tricarb 3180 TR/SL) after electrolytic enrichment at the Thailand Institute of Nuclear Technology (TINT). Sr analyses were performed on a Thermo-Finnigan Triton© TIMS at the Geoscience Centre at University of Göttingen (GZG, Germany). Prior to digestion, samples were mixed with a tracer solution enriched in ^{87}Rb-^{84}Sr.

Fig. 5. Vertical electrical sounding (VES, 1D) surveys in the study area and south of it: left: location of center, line direction, and max. AB/2 in meter; right: location of cross section 1 shown in Fig. 6.
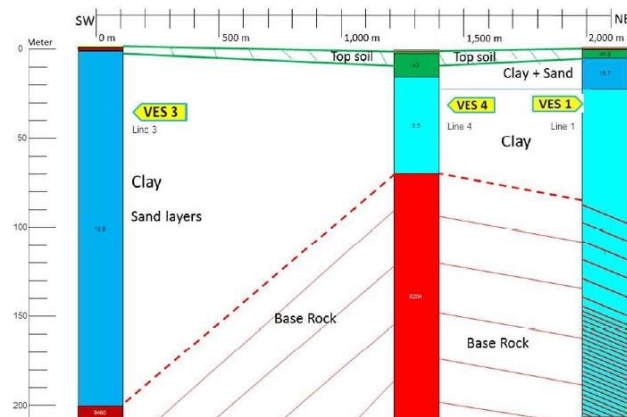
Fig. 6. Vertical electrical sounding (VES, 1D) surveys in the study area and south of it: Cross section comprising VES 3, 4, and 1 from SW to NE. Below the top soil is a low resistivity clay layer (with relatively thin sand layers). At the bottom is higher resistivity base rock (mud stone) increasing in depth from NE to SW over a short horizontal distance, thus requiring the introduction of a fault (see Fig. 7).
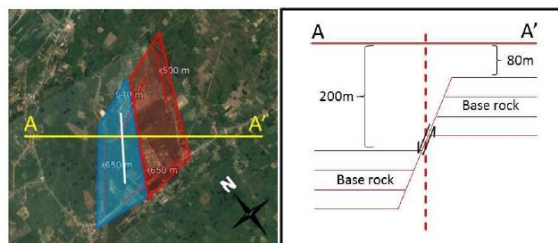
Fig. 7. Schematic cross section and possible fault orientation based on vertical electrical sounding (VES, 1D) surveys in the study area and south of it, see also Fig. 5 and 6.

Throughout this work a value of 0.710259±0.000076 (2σ) for the NBS 987 (n=4) was observed. Instrumental mass fractionation was corrected with $^{88}Sr/^{86}Sr$ of 0.1194 using exponential law.

Results and Discussion

Results show that the investigated groundwater can be classified in Na-Cl type for non-CO_2-rich groundwater (D1, D9) and in Na-Ca-HCO_3 type for CO_2-rich groundwater (D2, D4). The concentrations of the most cations (e.g. Ca, Mg, Na, K, Ba) and anions (e.g. Cl, SO4, HCO_3) including total dissolved solid (TDS) in CO_2-rich groundwater are significantly higher than that in non-CO_2-rich groundwater. In both CO_2-rich groundwater samples (D2 and D4) HCO_3 is the dominant anion (1,658 and 1,756 mg/L, respectively), followed by SO4 (122 and 110 mg/L, respectively).

Sr concentrations in CO_2-rich groundwater were relatively high, ranging from 1.30 to 1.37 µg/g. These concentrations are about 100 times higher than in non-CO_2-rich groundwater. The $^{87}Sr/^{86}Sr$ ratio of D2 and D4 showed a specific value of 0.726, whereas the $^{87}Sr/^{86}Sr$ ratios in the other waters ranged from 0.725 to 0.731. The high concentrations of ^3H were found in D1, D9 and surface water. The ^3H amount in soda groundwater was about four times lower than in non-soda groundwater. The $\delta^{13}C$ was significantly more depleted in D1, D9 and surface water than in D2 and D4. Sr concentrations and $^{87}Sr/^{86}Sr$ from well D9 ranged from 4.6 to 60.0 µg/g and 0.74118 to 0.776916 respectively.

Eu showed a positive anomaly ranging from 1.97 to 2.95 in non-CO_2-rich groundwater and exhibited a slightly negative anomaly in surface water. In contrast, the Eu anomaly of CO_2-rich groundwater was significantly positive with values of 32.38 and 72.26.

$\delta^{13}C$ values of CO_2-rich groundwater in this area ranging from -4.8 to -4.3‰ VPDB are in good agreement with the magmatic $\delta^{13}C$ values, which are normally characterized by $\delta^{13}C$ values between -10 and -3‰ VPDB [6]. Tritium amount close to zero

(0.29-0.38 TU) is an evidence of long residence time for water circulation exceeding 50 years. These hydrogeochemical and isotopic data indicate that the CO_2-rich groundwater was formed by the supply of deep-seated (magmatic) CO_2 at depth and rise along a fault system to the relatively shallow aquifers.

Geophysical VES results presented in Fig. 5-7 show higher resistivity bedrock at different depth, deeper in the SW part and shallower in the NE part south of the farm, thus indicating an extension of vertical faults under the farm. In some 2D resistivity sections (data not shown here) the resistivity distributions indicate vertical faults.

Conclusions

The CO2-rich groundwater in Khlong Hoi Khong in Songkhla Province, Thailand, can be characterized by its high HCO3, high TDS, and weak acidic to neutral pH. Based on the isotopic and hydrochemical data it can be concluded that the difference in CO2 content in the groundwater of this farm area can be interpreted to be the result of tectonic activities, probably during the basin development, with the migration of deep CO2-rich waters along fault systems up to shallower aquifers, where they accumulated as thicker clay layers acted as a seals prevented the CO2 to exit to the surface (Fig. 8; see also Fig. 1).
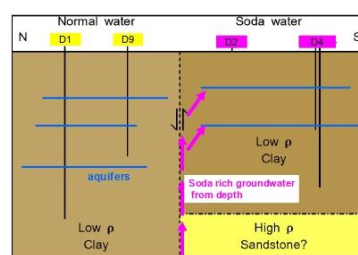
Fig. 8. Schematic drawing of the hydrogeological setting resulting in CO_2-rich groundwater occurrence in Songkhla.

Acknowledgment

References

[1] D.L. Thomas, D.K. Bird, S. Arnórsson, and K. Maher, "Geochemistry of CO_2-rich waters in Iceland," Chemical Geology, 444, 158-179, 2016.

[2] Y.K. Koh, B.Y. Choi, S.T. Yun, H.S. Choi, B. Mayer and S.W. Ryoo, "Origin and evolution of two contrasting thermal groundwaters (CO_2-rich and alkaline) in the Jungwon area, South Korea," Hydrochemical and isotopic evidence. Journal of Volcanology and Geothermal Research, 178(4), 777-786, 2008.

[3] E.K. Halland. "CO_2 Storage Atlas, Norwegian North Sea, Norway," Norwegian Petroleum Directorate, 2011.

[4] W. Lohawijarn, "Potential Ground Water Resources of Hat Yai Basin in Peninsular Thailand by Gravity Study." Songkhlanakarin Journal of Science and Technology 27(3), 633-647, 2005.

[5] A. Wattanathum, T. Chalermyanont, P. Sompongchaiyakul and S. Piromlert, "Numerical groundwater flow model for Hat Yai Basin, Songkhla Province, Thailand: a conceptual model," In the Proceeding of the 3rd National Environmental Conference. Hat Yai, Songkhla, 2004.

[6] DMR, Department of Mineral Resources, Geological Map of Ban Khlong Ngae Quadrangle, 2006.

[7] I.D. Clark and P. Fritz, "Environmental Isotopes in Hydrogeology". USA, CRC Press. 328 p, 1954.

VITAE

Name   Miss Poonnapa Klamthim

Student ID   6010220043

Educational Attainment

Degree	Name of Institution	Year of Graduation
Bachelor of Science (Physics)	Prince of Songkla University	2016

Scholarship Awards during Enrolment

Development and Promotion for Science and Technology talents project

List of Publications and Proceedings

Klamthim, P. and Duerrast, H., 2022. Geochemical Signatures of Hot Springs in Southern Thailand, The 3rd International Conference On Natural Sciences, Mathematics, Applications, Research, and Technology (ICON SMART 2022), Bali, 3-4 June.

Klamthim, P., Duerrast, H., Hengsuwan, M., 2019. Delineation of Unconventional Groundwater: I. Soda Groundwater in Songkhla, Thailand. THA 2019 International Conference, Thailand, 23-25 January.